Numerical Homogenization of Trabecular Bone Specimens using Composite Finite Elements

Lars Ole Schwen

Institute for Numerical Simulation
University of Bonn

Joint work with: Martin Rumpf (INS Bonn)
Tobias Preusser (MEVIS Bremen)
Hans-Joachim Wilke, Uwe Wolfram (UFB Ulm)
Stefan Sauter (Uni Zürich)

CdE-Seminar 2010
Siegburg, 2010–11–27

Preview: Effective Elasticity Tensors

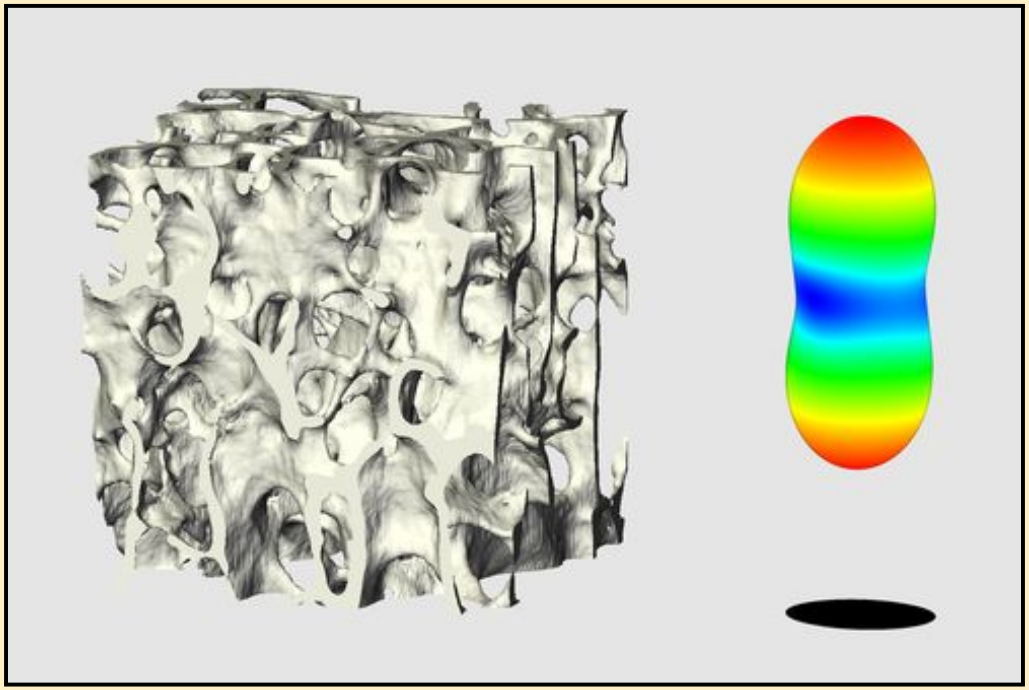

Goal: for ‘representative cells’ of trabecular structures, determine effective elasticity properties

Outline

Contents

Numerical Homogenization (Exactly Periodic Case)

Determine effective elasticity tensor by imposing different unit strains and computing stress response.

Numerical Homogenization (Exactly Periodic Case)

Determine effective elasticity tensor by imposing different unit strains and computing stress response.

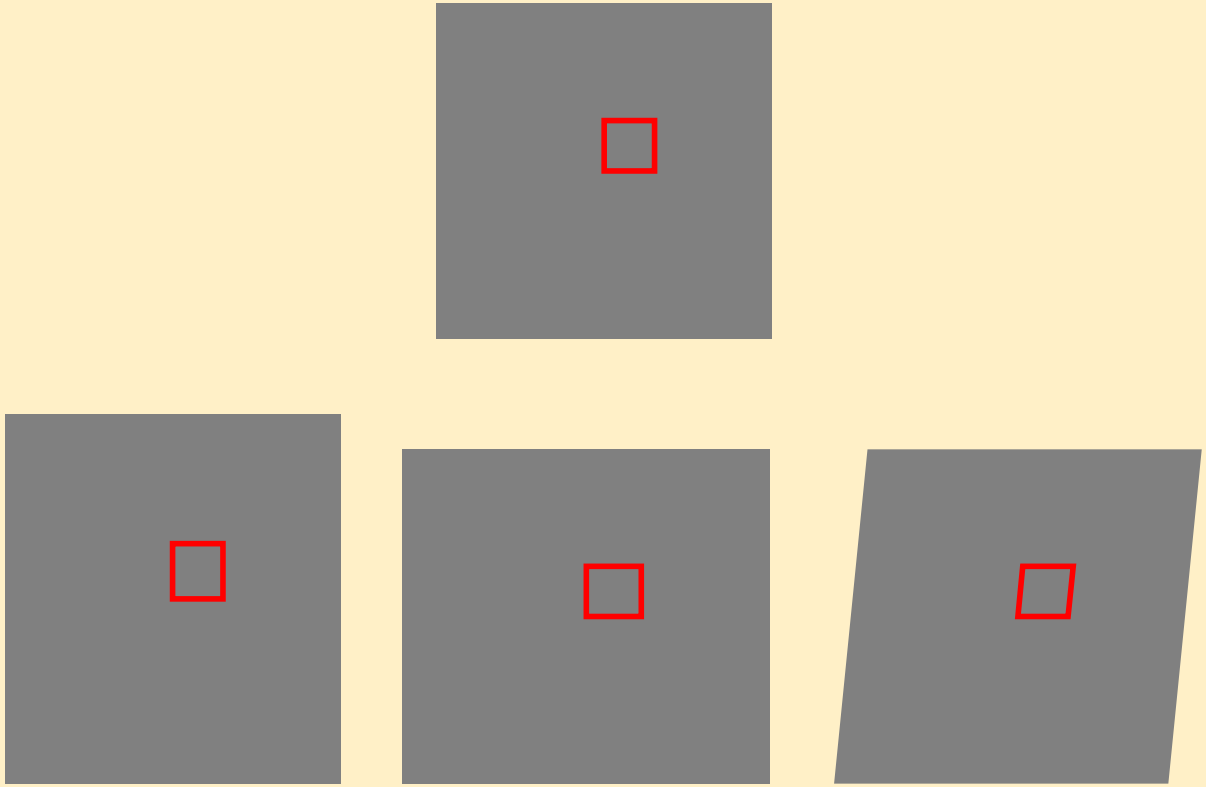

Cell Problems, anyone?

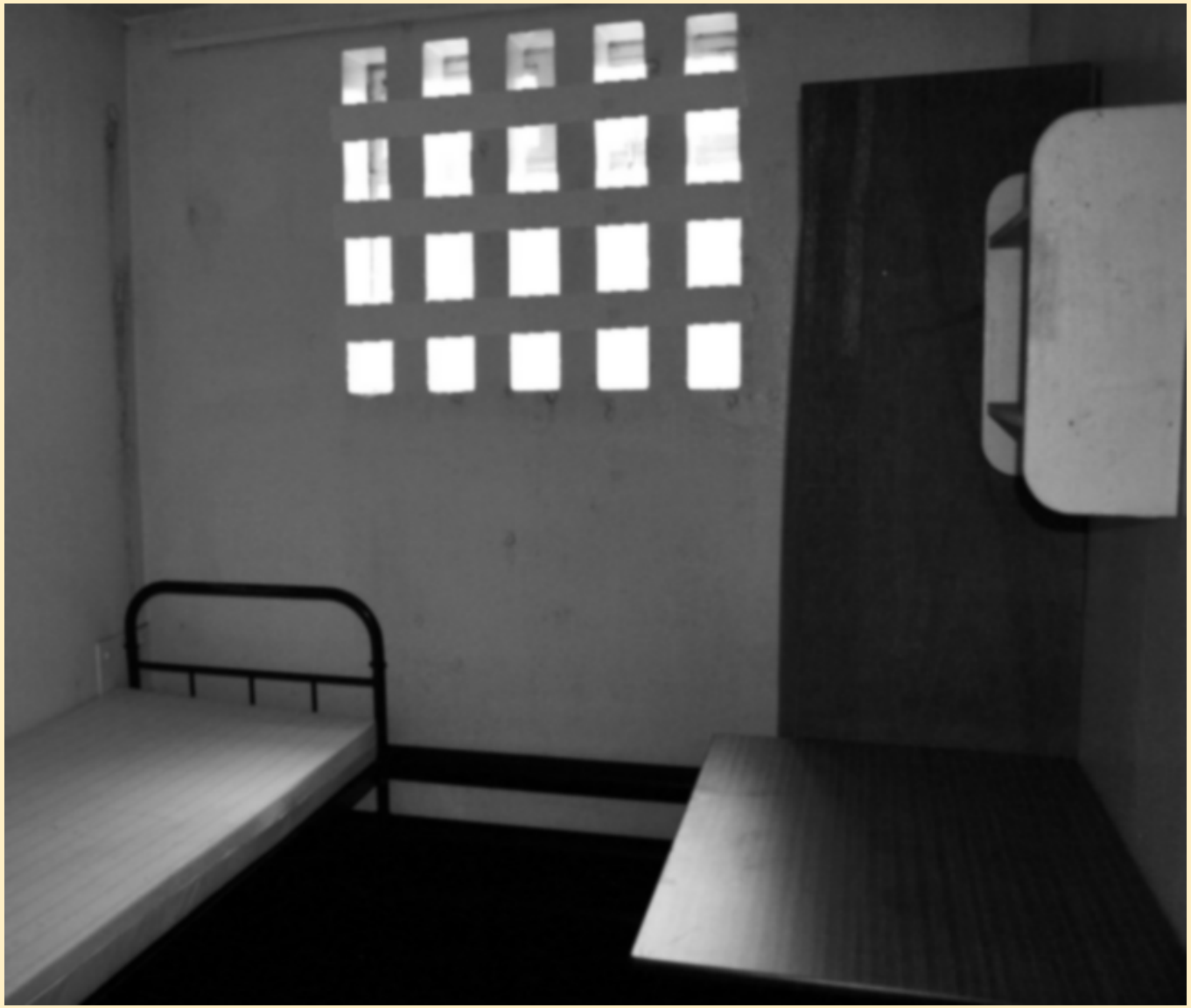

adapted from an image by “Still Burning” on flickr.com

Cell Problems, anyone?

adapted from an image by “Lynda & Leonard” on picasaweb.google.com

Numerical Homogenization (Exactly Periodic Case)

Decompose physical displacement $u = \bar{u} + \tilde{u}$ in

- macroscopic unit strain $\bar{u}$ and
- oscillatory periodic correction profile $\tilde{u}$

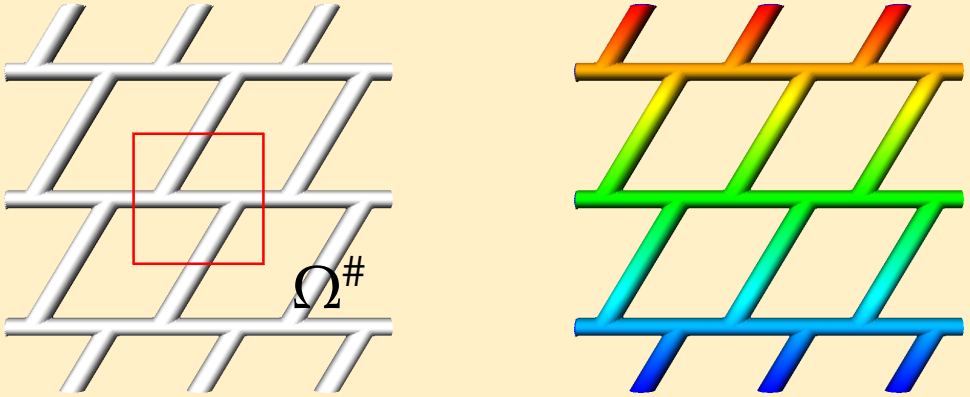

Numerical Homogenization (Exactly Periodic Case)

Decompose physical displacement $u = \bar{u} + \tilde{u}$ in

- macroscopic unit strain $\bar{u}$ and
- oscillatory periodic correction profile $\tilde{u}$

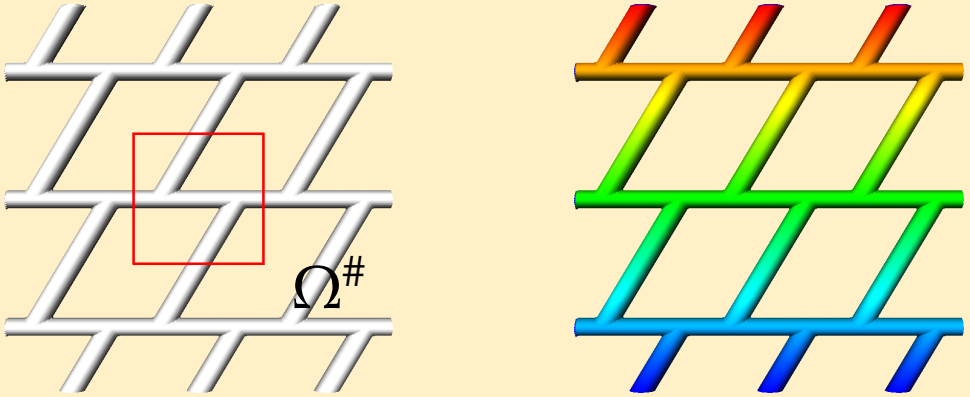

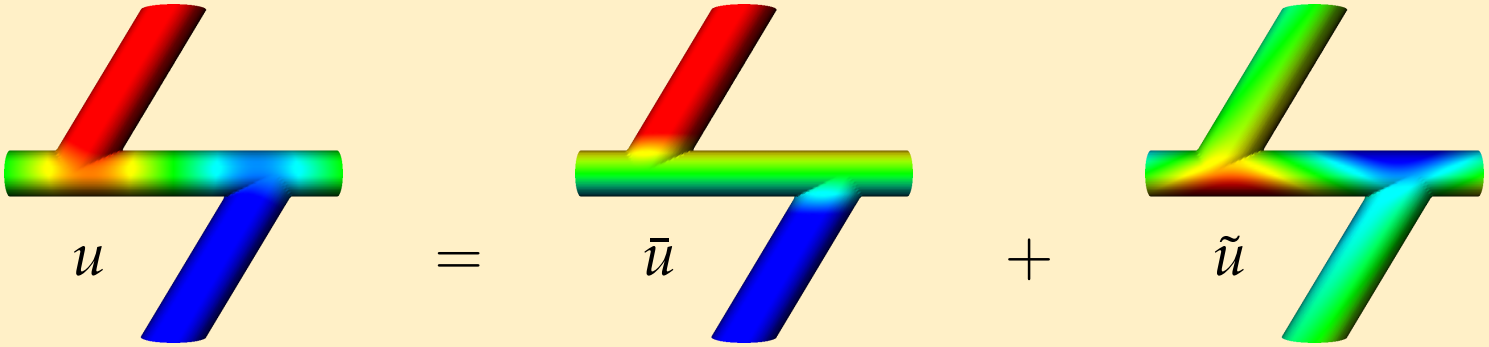

z displacement

Numerical Homogenization (Exactly Periodic Case)

Decompose physical displacement $u = \bar{u} + \tilde{u}$ in

- macroscopic unit strain $\bar{u}$ and
- oscillatory periodic correction profile $\tilde{u}$

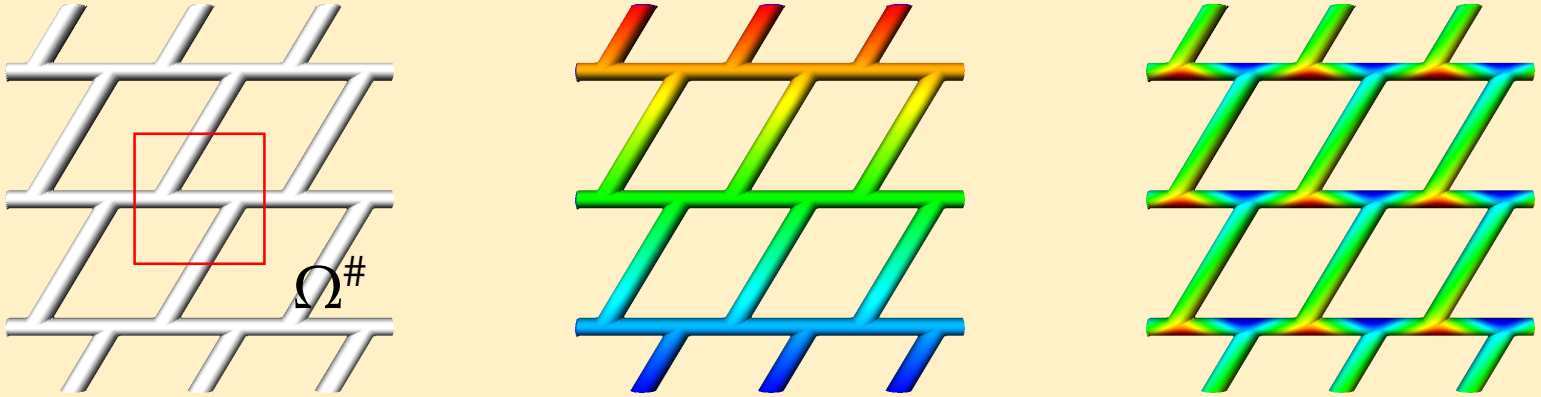

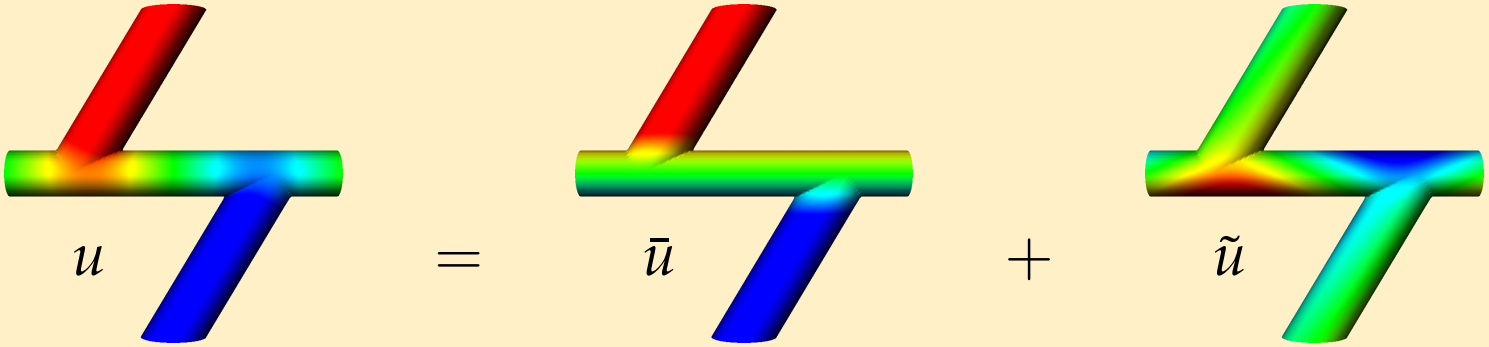

z displacement

Numerical Homogenization (Exactly Periodic Case)

Decompose physical displacement $u = \bar{u} + \tilde{u}$ in

- macroscopic unit strain $\bar{u}$ and
- oscillatory periodic correction profile $\tilde{u}$

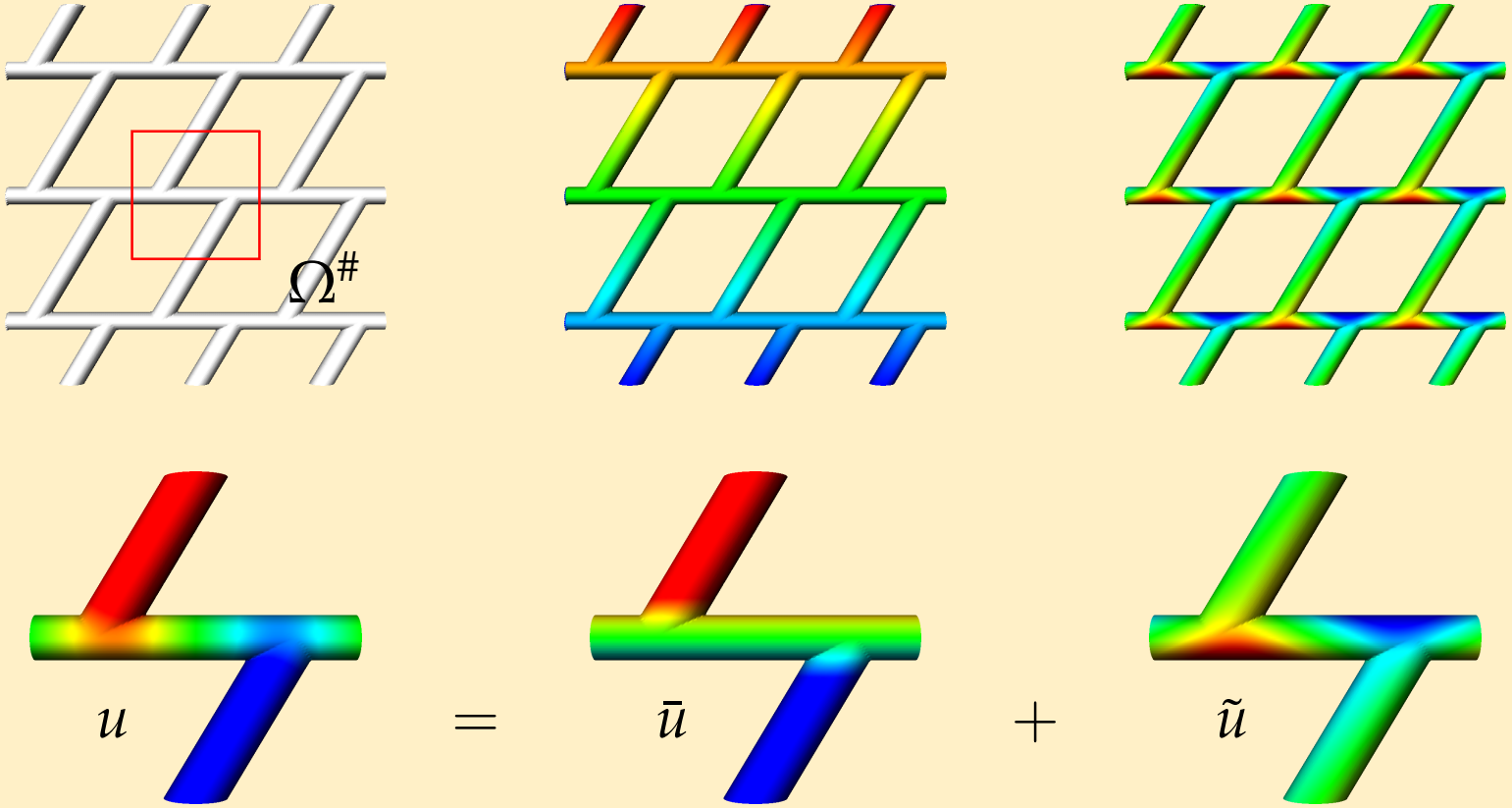

Let's make this more precise ...

z displacement

Linearized Elasticity Model

Microscopic material parameters (isotropic):

- Young's modulus (stiffness) $E = 13$ GPa
- Poisson's ratio (bulging ratio) $\nu = 0.32$

[Wolfram, Wilke, Zysset Bone 46:348]

Linearized Elasticity Model

Microscopic material parameters (isotropic):

- Young's modulus (stiffness) $E = 13$ GPa
- Poisson's ratio (bulging ratio) $\nu = 0.32$

[Wolfram, Wilke, Zysset Bone 46:348]

Displacement $u : \Omega^{\#} \to \mathbb{R}^3$

Elasticity tensor C couples

- strain $\epsilon(u) = \frac{1}{2}\left[\nabla u + (\nabla u)^T\right]$
- and stress σ via $\sigma = C\epsilon(u)$

Linearized Elasticity Model

Microscopic material parameters (isotropic):

- Young's modulus (stiffness) $E = 13$ GPa
- Poisson's ratio (bulging ratio) $\nu = 0.32$

[Wolfram, Wilke, Zysset Bone 46:348]

Displacement $u : \Omega^{\#} \to \mathbb{R}^3$

Elasticity tensor C couples

- strain $\epsilon(u) = \frac{1}{2}\left[\nabla u + (\nabla u)^T\right]$
- and stress σ via $\sigma = C\epsilon(u)$

Leading to PDE

$$-\operatorname{div} C\epsilon(u) = f$$

where f is neglected.

Numerical Homogenization (Exactly Periodic Case)

Decompose physical displacement $u = \bar{u} + \tilde{u}$ in

- macroscopic strain $\bar{u}$ (given) and
- oscillatory periodic correction profile $\tilde{u}$ (unknown)

Elasticity equation:

$$\begin{aligned} & -\operatorname{div} C\epsilon(u) = 0 \\ \Rightarrow\ & -\operatorname{div} C\epsilon(\tilde{u}) = \operatorname{div} C\epsilon(\bar{u}) \end{aligned}$$

To ensure uniqueness of the decomposition, require $\fint_{\Omega^\#} \tilde{u} = 0$.

Numerical Homogenization (Exactly Periodic Case)

Decompose physical displacement $u = \bar{u} + \tilde{u}$ in

- macroscopic strain $\bar{u}$ (given) and
- oscillatory periodic correction profile $\tilde{u}$ (unknown)

Elasticity equation:

$$\begin{aligned} -\operatorname{div} C\epsilon(u) &= 0 \\ \Rightarrow\ -\operatorname{div} C\epsilon(\tilde{u}) &= \operatorname{div} C\epsilon(\bar{u}) \end{aligned}$$

To ensure uniqueness of the decomposition, require $\fint_{\Omega^\#} \tilde{u} = 0$.

For $\bar{u}^{ij}$ with $\epsilon(\bar{u}^{ij}) = e_{ij} := \frac{1}{2}(e_i \otimes e_j + e_j \otimes e_i)$, compute $\tilde{u}^{ij}$

Numerical Homogenization (Exactly Periodic Case)

Decompose physical displacement $u = \bar{u} + \tilde{u}$ in

- macroscopic strain $\bar{u}$ (given) and
- oscillatory periodic correction profile $\tilde{u}$ (unknown)

Elasticity equation:

$$\begin{aligned} &-\operatorname{div} C\epsilon(u) = 0 \\ \Rightarrow\ &-\operatorname{div} C\epsilon(\tilde{u}) = \operatorname{div} C\epsilon(\bar{u}) \end{aligned}$$

To ensure uniqueness of the decomposition, require $\fint_{\Omega^\#} \tilde{u} = 0$.

For $\bar{u}^{ij}$ with $\epsilon(\bar{u}^{ij}) = e_{ij} := \frac{1}{2}(e_i \otimes e_j + e_j \otimes e_i)$, compute $\tilde{u}^{ij}$ and due to $\sigma = C\epsilon$ obtain

$$\bar{C}_{..ij} = \bar{\sigma}^{ij} = \fint_{\Omega^\#} C\Big[\underbrace{\epsilon(\bar{u}^{ij})}_{e_{ij}} + \epsilon(\tilde{u}^{ij})\Big]$$

Numerical Homogenization (Statistically Periodic Case)

In case of non-periodic microstructures, need statistically representative fundamental cell of at least 5 inter-trabecular distances [Harrigan et al, JBiomech 21:269].

Numerical Homogenization (Statistically Periodic Case)

In case of non-periodic microstructures, need statistically representative fundamental cell of at least 5 inter-trabecular distances [Harrigan et al, JBiomech 21:269].

Problem: cannot enforce periodic boundary conditions.

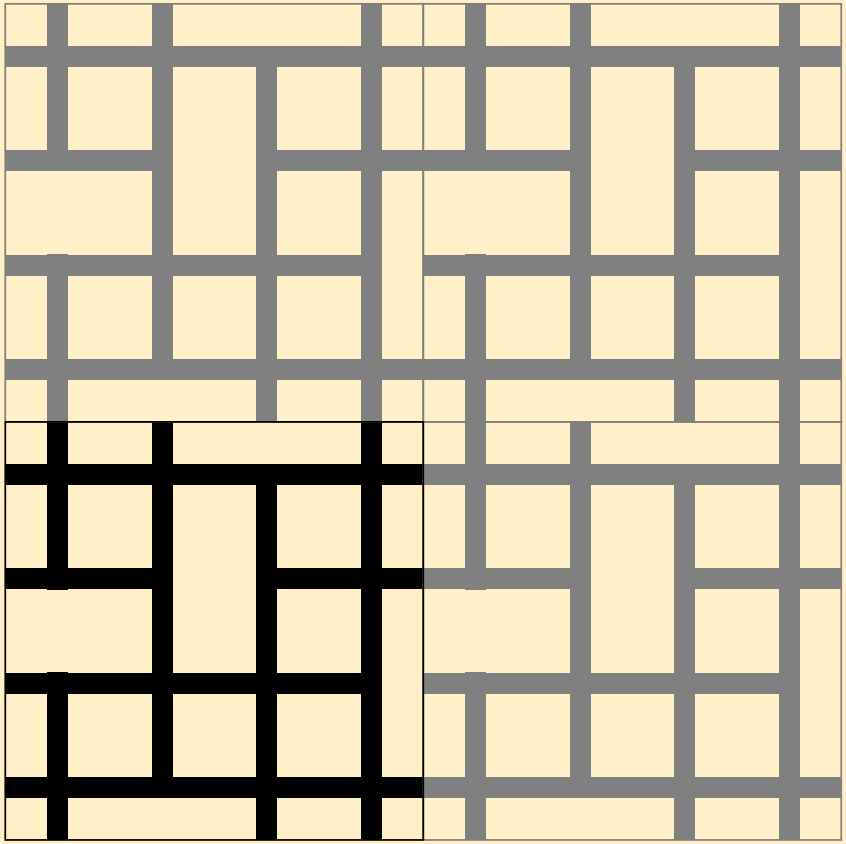

Numerical Homogenization (Statistically Periodic Case)

In case of non-periodic microstructures, need statistically representative fundamental cell of at least 5 inter-trabecular distances [Harrigan et al, JBiomech 21:269].

Could make structure periodic by mirroring

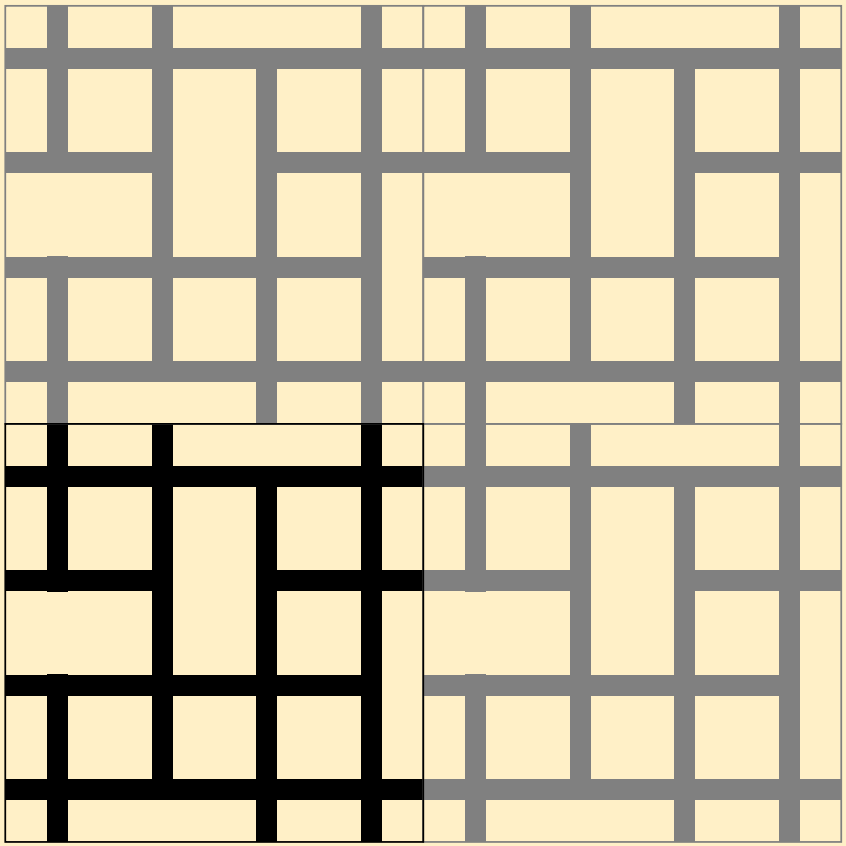

Numerical Homogenization (Statistically Periodic Case)

In case of non-periodic microstructures, need statistically representative fundamental cell of at least 5 inter-trabecular distances [Harrigan et al, JBiomech 21:269].

Could make structure periodic by mirroring

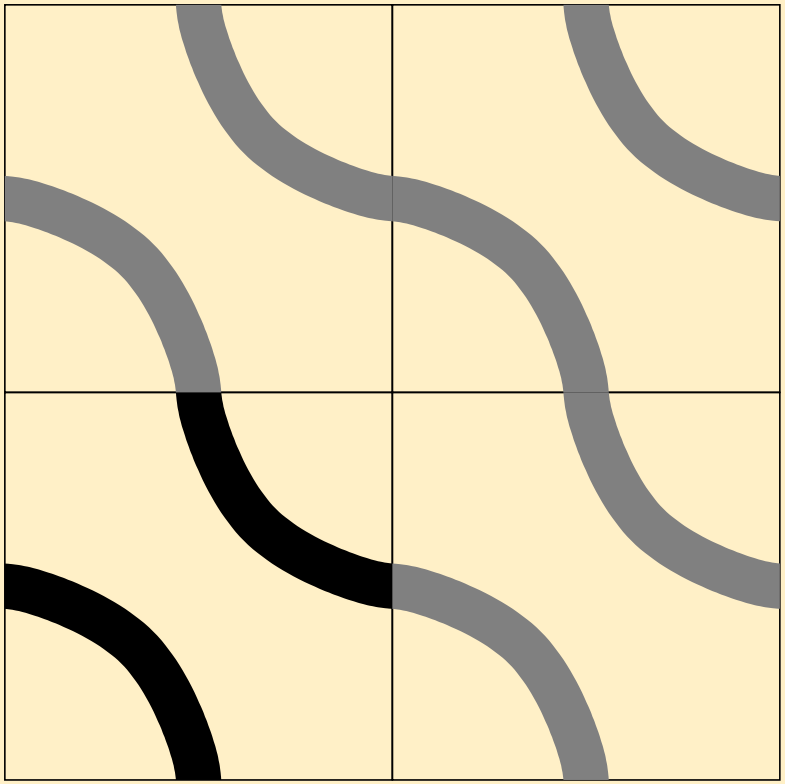

Numerical Homogenization (Statistically Periodic Case)

In case of non-periodic microstructures, need statistically representative fundamental cell of at least 5 inter-trabecular distances [Harrigan et al, JBiomech 21:269].

Could make structure periodic by mirroring, but that is a bad idea.

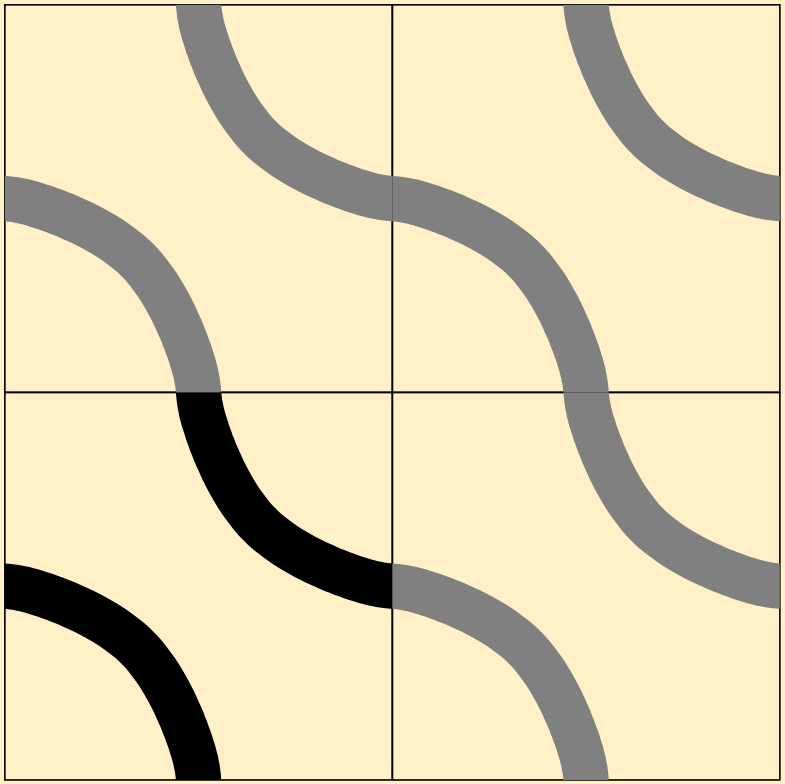

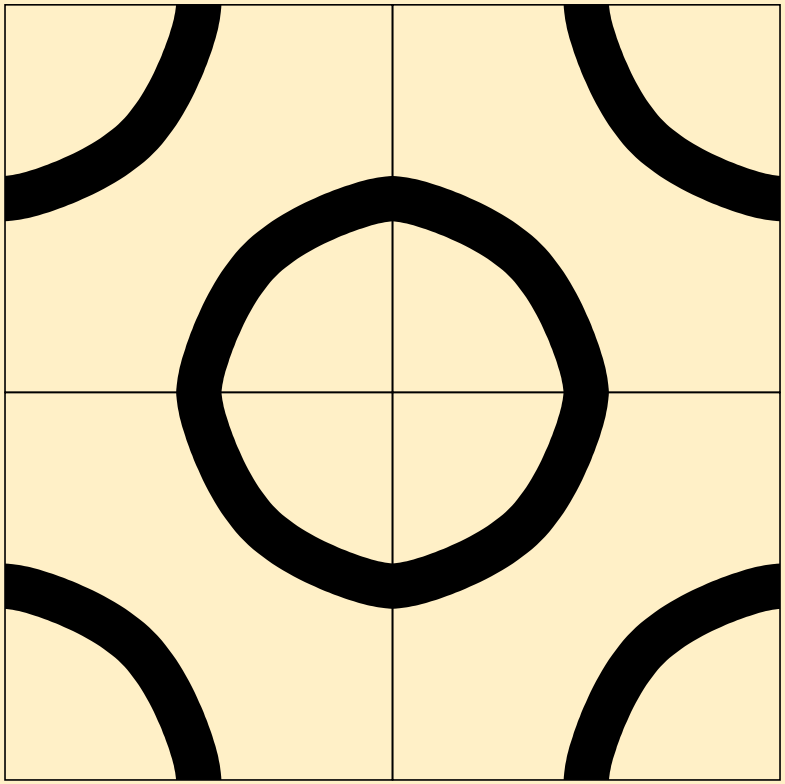

Numerical Homogenization (Statistically Periodic Case)

Idea: Enforce macroscopic strain by displacement (Dirichlet) boundary conditions on $\partial^{\square}\Omega^{\#}$.

Numerical Homogenization (Statistically Periodic Case)

Idea: Enforce macroscopic strain by displacement (Dirichlet) boundary conditions on $\partial^{\square}\Omega^{\#}$.

For $\bar{u}^{ij} = e_{ij} := \frac{1}{2}(e_i \otimes e_j + e_j \otimes e_i)$ (as before), consider

$$\begin{aligned} -\operatorname{div}\left(C\epsilon(u^{ij})\right) &= 0 \quad \text{in } \Omega^{\#} \\ u^{ij} &= \bar{u}^{ij} \quad \text{on } \partial^{\square}\Omega^{\#} \end{aligned}$$

Numerical Homogenization (Statistically Periodic Case)

Idea: Enforce macroscopic strain by displacement (Dirichlet) boundary conditions on $\partial^{\square}\Omega^{\#}$.

For $\bar{u}^{ij} = e_{ij} := \frac{1}{2}(e_i \otimes e_j + e_j \otimes e_i)$ (as before), consider

$$\begin{aligned} -\operatorname{div}\left(C\epsilon(u^{ij})\right) &= 0 \quad && \text{in } \Omega^{\#} \\ u^{ij} &= \bar{u}^{ij} \quad && \text{on } \partial^{\square}\Omega^{\#} \end{aligned}$$

The average stress is then evaluated as

$$\left[\bar{C}_{ij\cdot\cdot} = \right]\bar{\sigma}^{ij} = \fint_{\Omega^{\#}_{\beta}} C\epsilon[u^{ij}]\,.$$

Numerical Homogenization (Statistically Periodic Case)

Idea: Enforce macroscopic strain by displacement (Dirichlet) boundary conditions on $\partial^{\square}\Omega^{\#}$.

For $\bar{u}^{ij} = e_{ij} := \frac{1}{2}(e_i \otimes e_j + e_j \otimes e_i)$ (as before), consider

$$\begin{aligned} -\operatorname{div}\left(C\epsilon(u^{ij})\right) &= 0 \quad \text{in } \Omega^{\#} \\ u^{ij} &= \bar{u}^{ij} \quad \text{on } \partial^{\square}\Omega^{\#} \end{aligned}$$

The average stress is then evaluated as

$$\left[\bar{C}_{ij\cdot\cdot} = \right]\bar{\sigma}^{ij} = \fint_{\Omega^{\#}_{\beta}} C\epsilon[u^{ij}]\,.$$

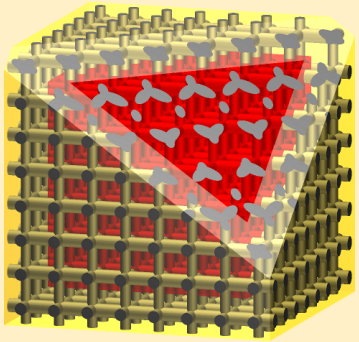

$\Omega^{\#}_{\beta} = \{x \in \Omega^{\#} \mid \operatorname{dist}(x, \partial^{\square}\Omega^{\#} > \beta\}$. Why?

Numerical Homogenization (Statistically Periodic Case)

Problem: artificial stiffening near the boundary by enforcing displacement boundary conditions (right)

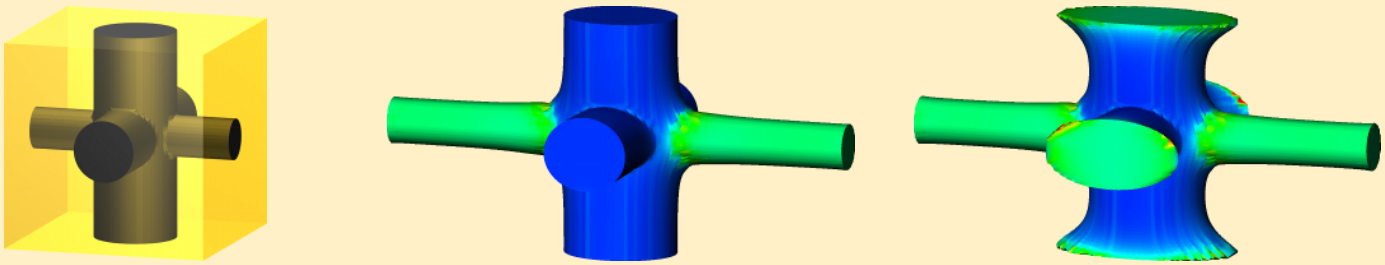

Numerical Homogenization (Statistically Periodic Case)

Problem: artificial stiffening near the boundary by enforcing displacement boundary conditions (right)

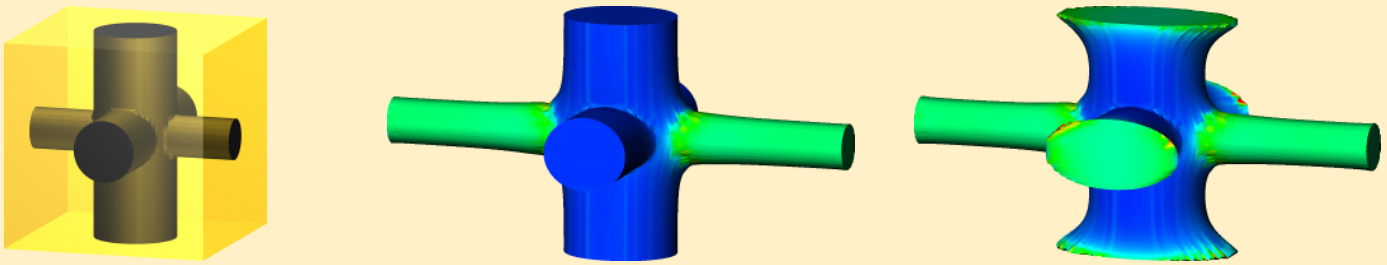

Solution: ignore boundary layer and
evaluate stress only in interior $\Omega_\beta^\#$ (typically $\beta = 0.125$)

cf. [Ün, Bevill, Keaveny J Biomech 39:1955]

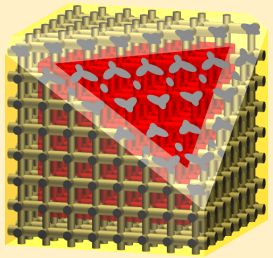

Note that $\Omega_\beta^\#$ still needs to be representative.

Visualization of Elasticity Tensors

Tensors are visualized as deformed (encoding uniaxial stiffness) and colored (encodes bulk modulus) spheres.

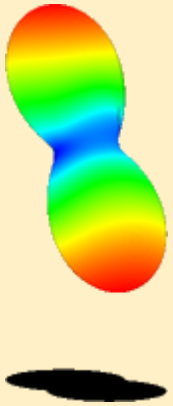

Visualization of Elasticity Tensors

Tensors are visualized as deformed (encoding uniaxial stiffness) and colored (encodes bulk modulus) spheres.

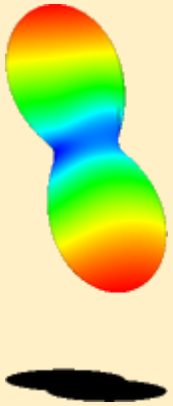

Orthotropy? Axes of orthotropy?

Optimal Tensor Rotation

Determine rotation matrix $Q \in \mathrm{SO}(3)$ (with angle bound) minimizing orthotropy violation

$$F_{\bar{C}}(Q) = \frac{\|R_a[\bar{C}^Q]\|_{\mathrm{F}}^2}{\|R_b[\bar{C}^Q]\|_{\mathrm{F}}^2} \quad \text{where } \bar{C}^Q := Q_{mi}Q_{nj}Q_{pk}Q_{ql}\bar{C}_{ijkl}$$

Optimal Tensor Rotation

Determine rotation matrix $Q \in \mathrm{SO}(3)$ (with angle bound) minimizing orthotropy violation

$$F_{\bar{C}}(Q) = \frac{\|R_a[\bar{C}^Q]\|_F^2}{\|R_b[\bar{C}^Q]\|_F^2} \quad \text{where } \bar{C}^Q := Q_{mi}Q_{nj}Q_{pk}Q_{ql}\bar{C}_{ijkl}$$

$$\bar{C} = \begin{bmatrix} 0.3926 & 0.1726 & 0.1771 & -0.0013 & -0.0088 & -0.0304 \\ 0.1726 & 0.3678 & 0.1804 & -0.0010 & 0.0073 & -0.0108 \\ 0.1771 & 0.1804 & 1.0276 & -0.0111 & 0.0218 & -0.0032 \\ -0.0013 & -0.0010 & -0.0111 & 0.1668 & -0.0305 & 0.0064 \\ -0.0088 & 0.0073 & 0.0218 & -0.0305 & 0.1718 & -0.0022 \\ -0.0304 & -0.0108 & -0.0032 & 0.0064 & -0.0022 & 0.0907 \end{bmatrix}$$

Optimal Tensor Rotation

Determine rotation matrix $Q \in \mathrm{SO}(3)$ (with angle bound) minimizing orthotropy violation

$$F_{\bar{C}}(Q) = \frac{\|R_a[\bar{C}^Q]\|_F^2}{\|R_b[\bar{C}^Q]\|_F^2} \quad \text{where } \bar{C}^Q := Q_{mi}Q_{nj}Q_{pk}Q_{ql}\bar{C}_{ijkl}$$

$$\bar{C}^Q = \begin{bmatrix} 0.4090 & 0.1856 & 0.1809 & -0.0039 & -0.0018 & 0.0164 \\ 0.1856 & 0.3260 & 0.1749 & 0.0004 & -0.0051 & -0.0045 \\ 0.1809 & 0.1749 & 1.0302 & 0.0018 & 0.0016 & -0.0027 \\ -0.0039 & 0.0004 & 0.0018 & 0.1380 & 0.0005 & -0.0073 \\ -0.0018 & -0.0051 & 0.0016 & 0.0005 & 0.1988 & -0.0059 \\ 0.0164 & -0.0045 & -0.0027 & -0.0073 & -0.0059 & 0.1038 \end{bmatrix}$$

Contents

1D Discretization

Continuous (temperature) profile

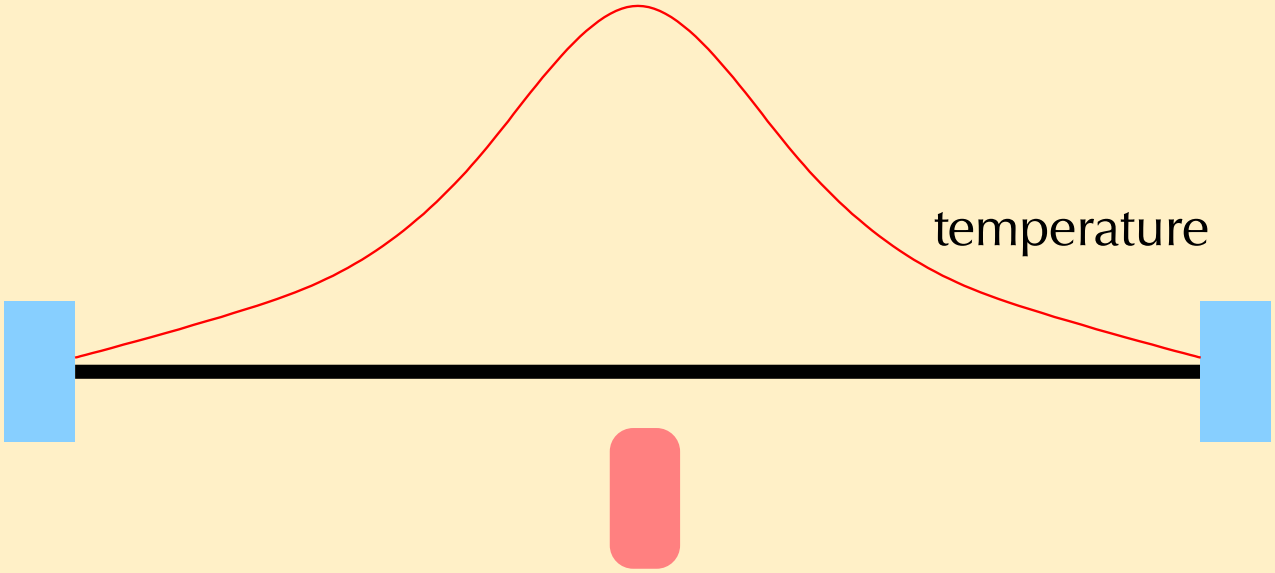

1D Discretization

Continuous (temperature) profile

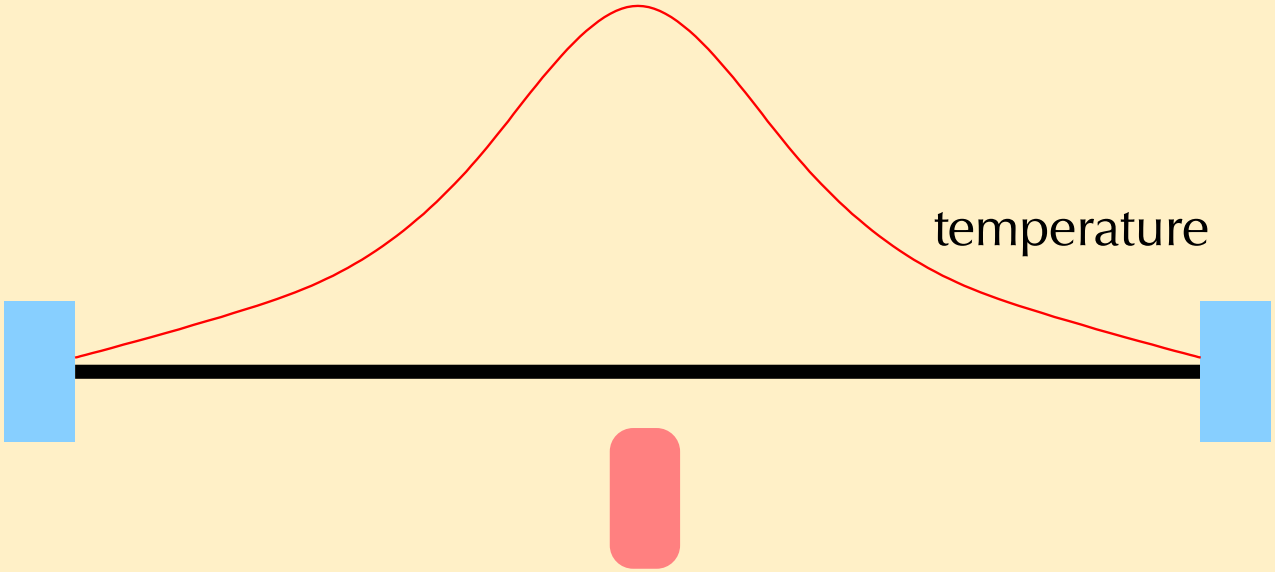

is approximated

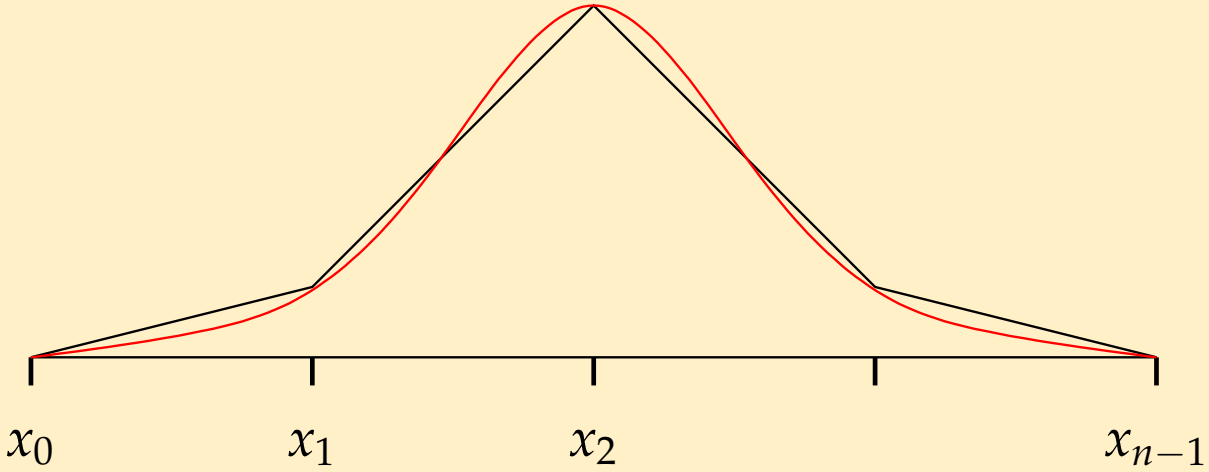

1D Discretization

Continuous (temperature) profile

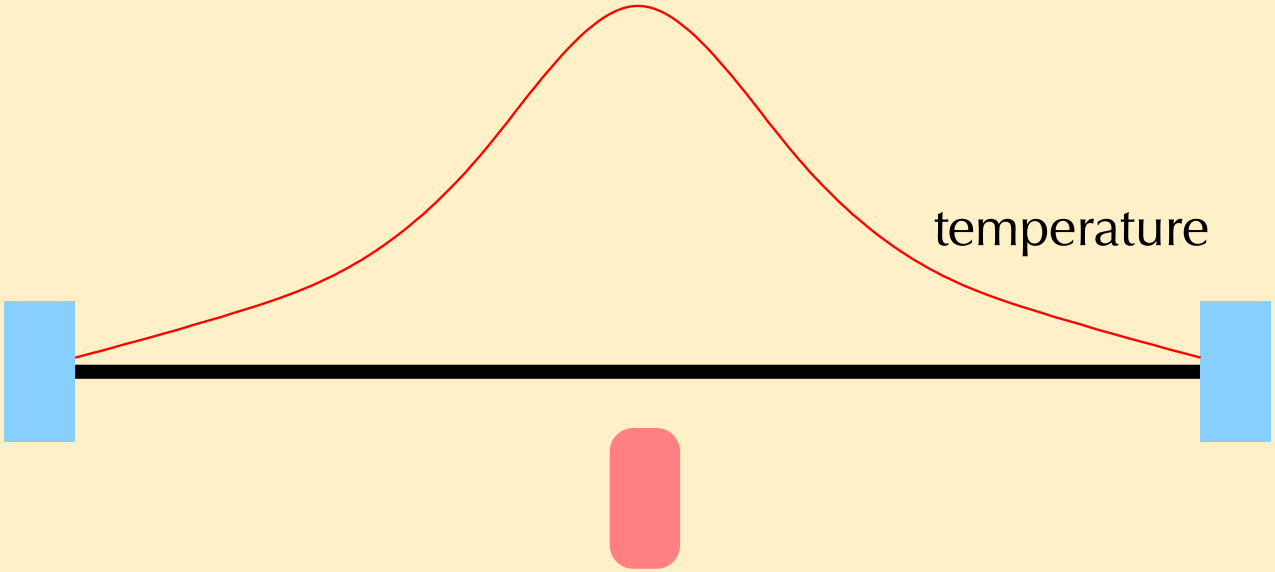

is approximated

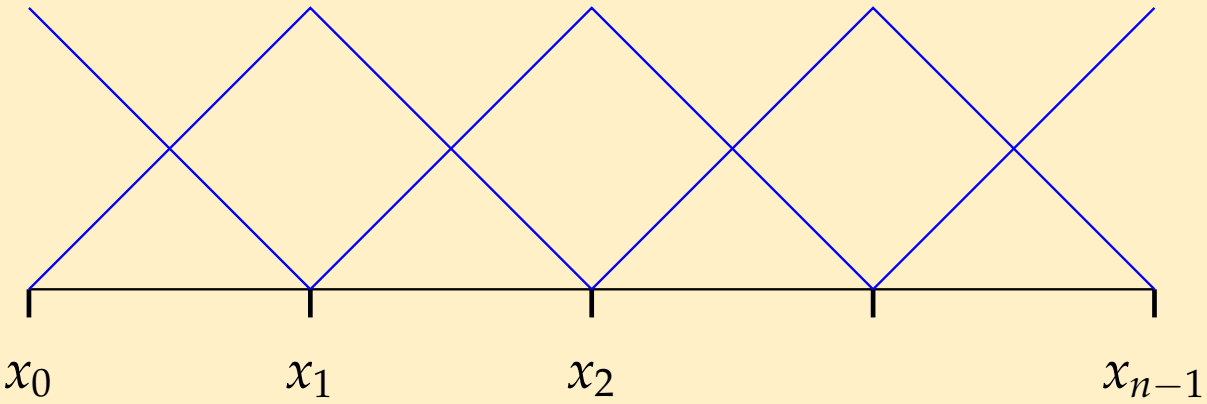

1D Discretization

Continuous (temperature) profile

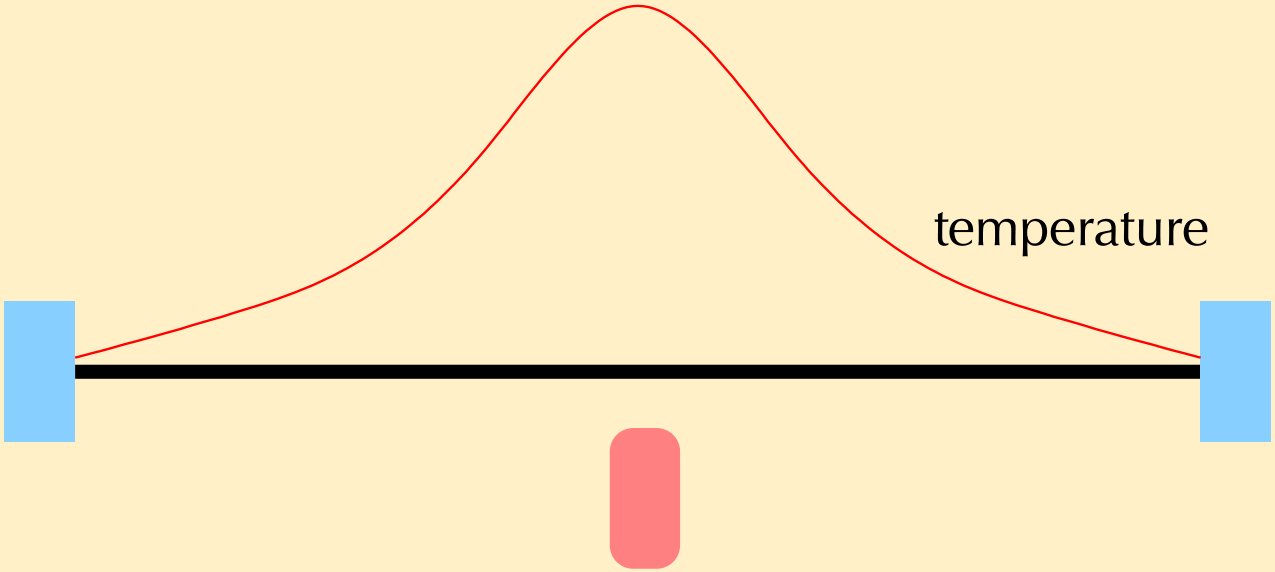

is approximated

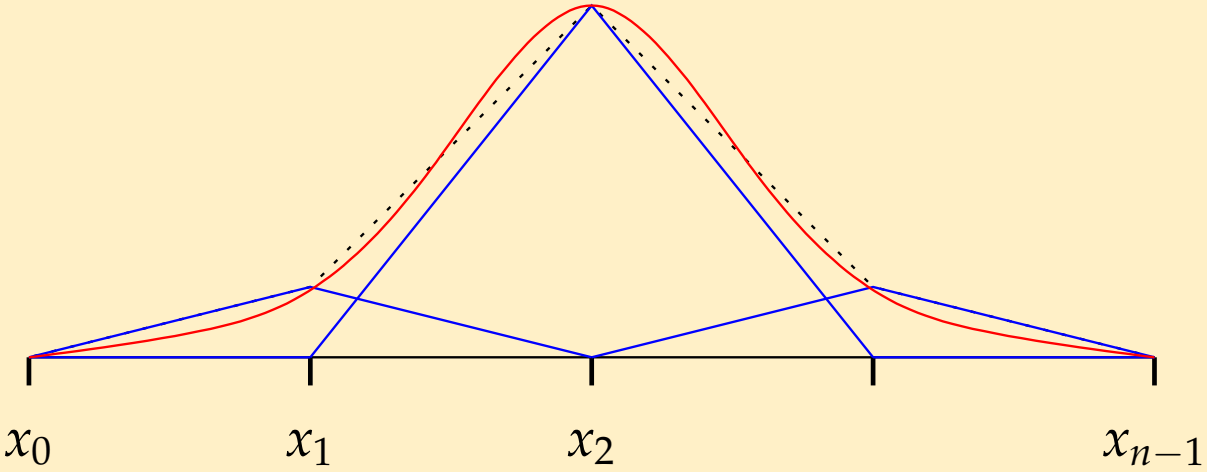

Composite Finite Elements in 1D

- ‘complicated’ domain (dashed) with DOF on uniform grid

Composite Finite Elements in 1D

- ‘complicated’ domain (dashed) with DOF on uniform grid

- ‘virtual’ tent basis with additional nodes

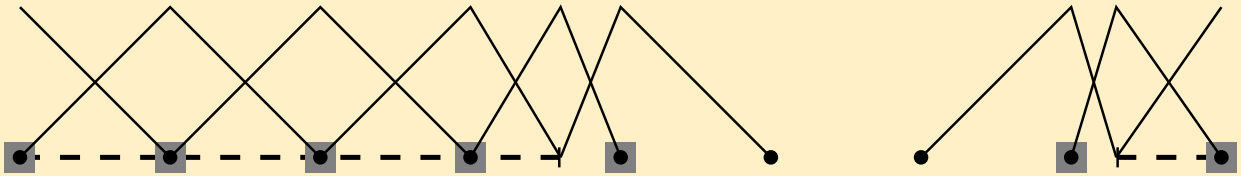

Composite Finite Elements in 1D

- ‘complicated’ domain (dashed) with DOF on uniform grid

- ‘virtual’ tent basis with additional nodes

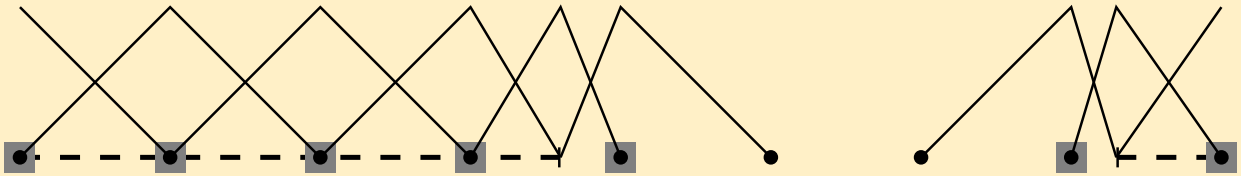

- weighted, restricted and composed to ‘CFE tents’

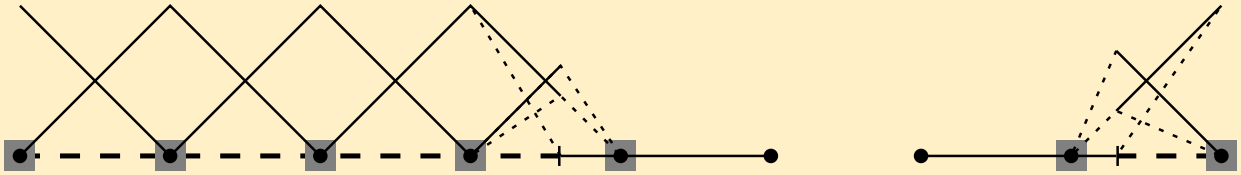

Composite Finite Elements in 1D

- ‘complicated’ domain (dashed) with DOF on uniform grid

- ‘virtual’ tent basis with additional nodes

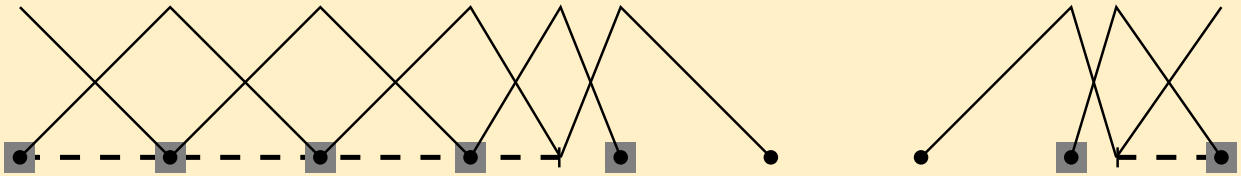

- weighted, restricted and composed to ‘CFE tents’

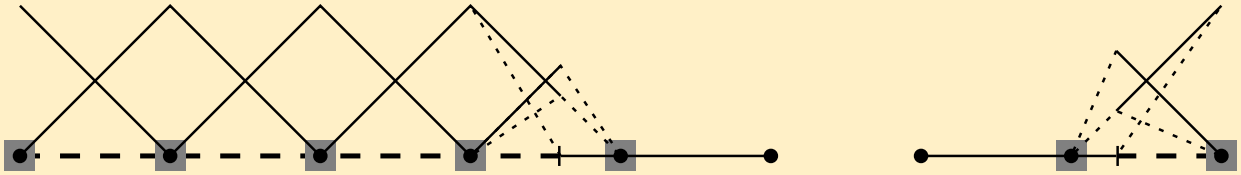

In 1D, this may seem to be a complicated solution for a simple problem . . .

Complicated domains in 2D

Interfaces in 2D:

Complicated domains in 2D

Interfaces in 2D:

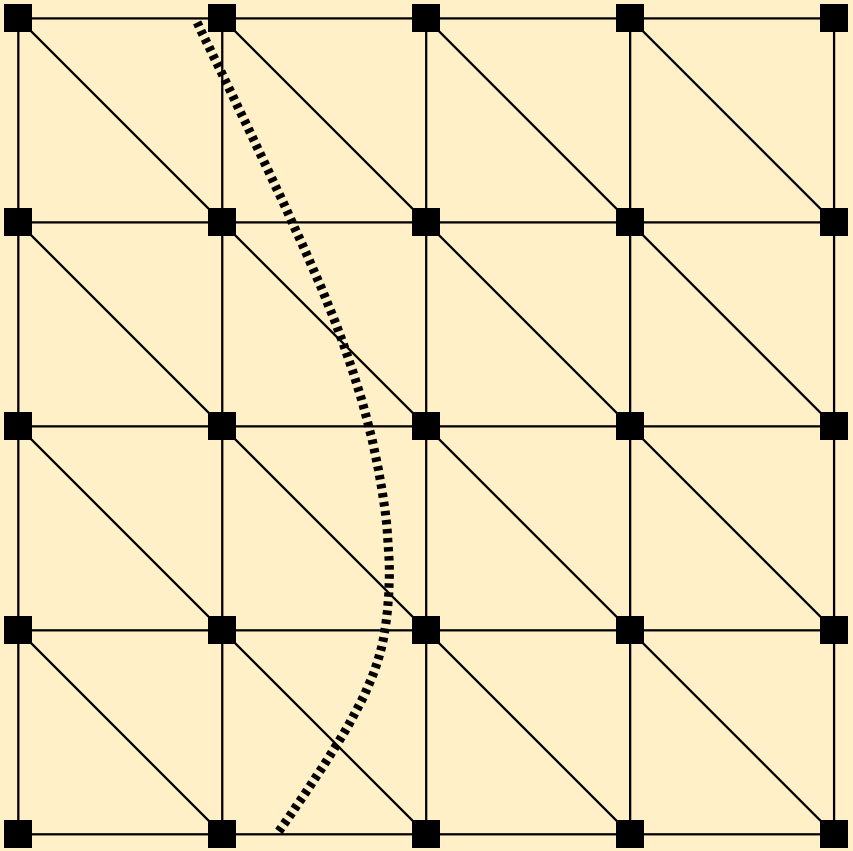

- could use ‘virtual’ triangular mesh (poor quality)
- could generate better triangular mesh (expensive)

Complicated domains in 2D

Interfaces in 2D:

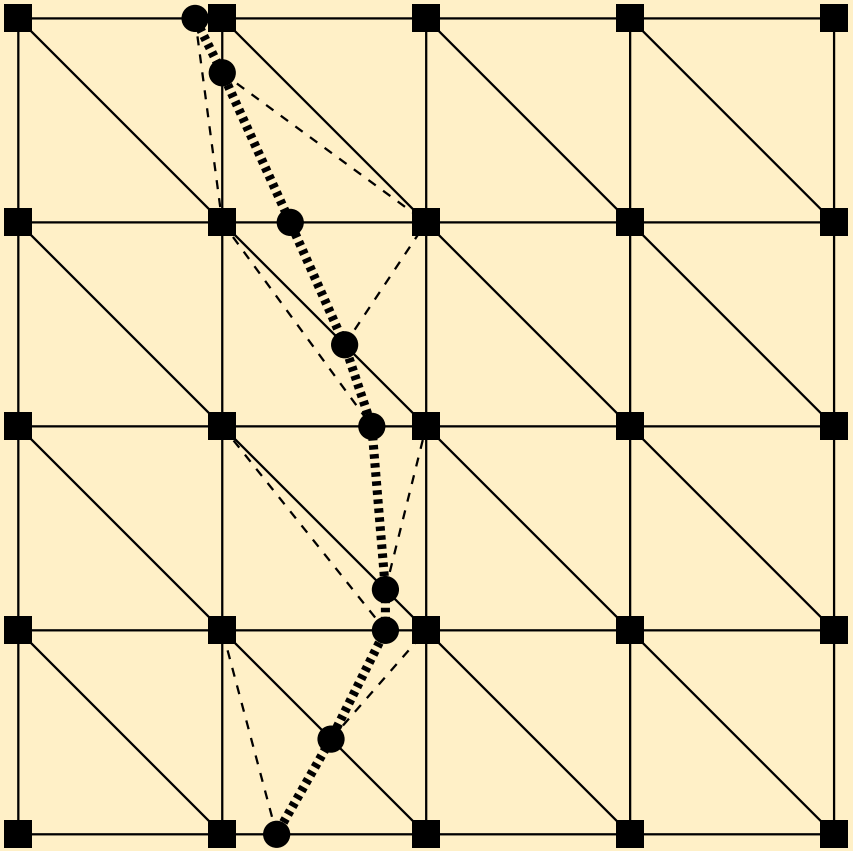

- could use ‘virtual’ triangular mesh (poor quality)
- could generate better triangular mesh (expensive)

CFE Basis Functions in 2D

[Hackbusch/Sauter; Liehr/Preusser/Rumpf/Sauter/S. Comp Vis Sci 12:171]

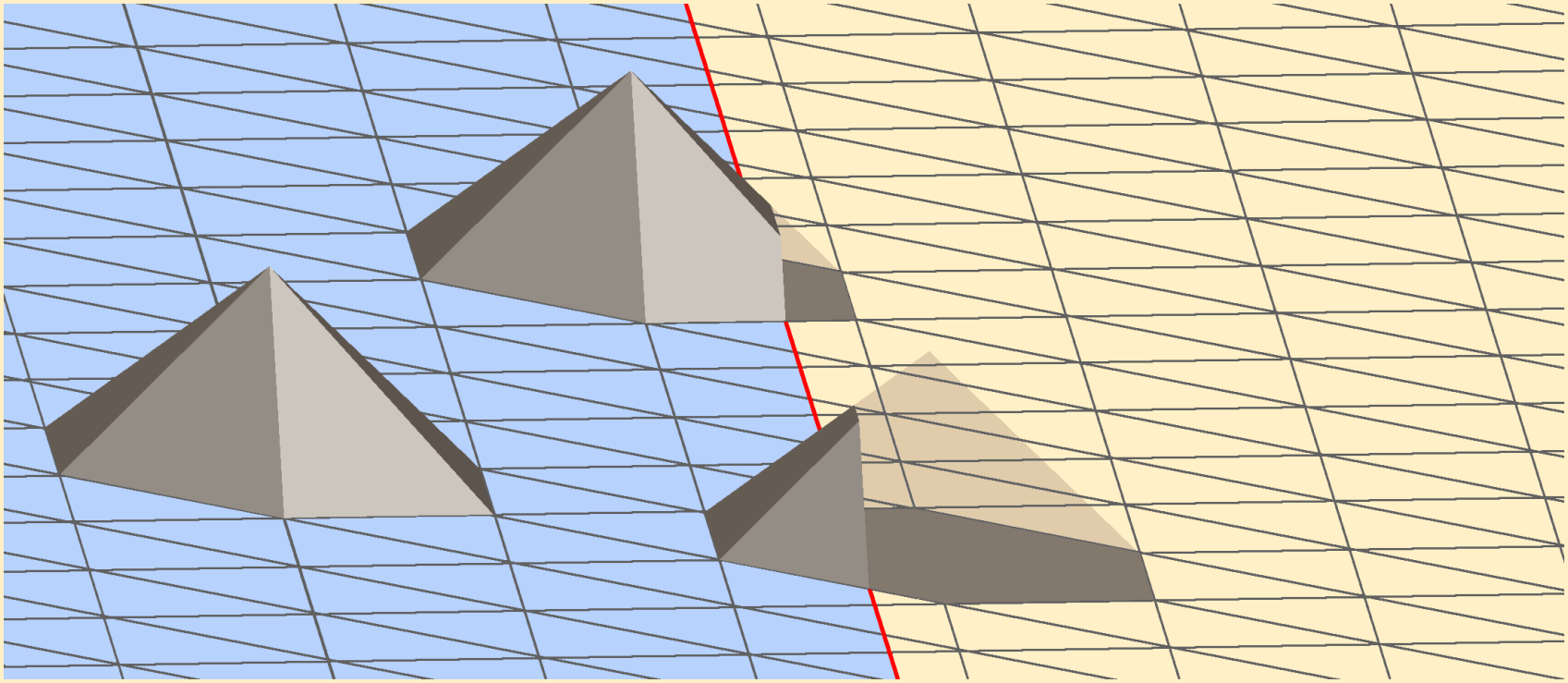

- far inside: standard tent
- at interface: truncated tent
- far outside: no tent

CFE Basis Functions in 2D

[Hackbusch/Sauter; Liehr/Preusser/Rumpf/Sauter/S. Comp Vis Sci 12:171]

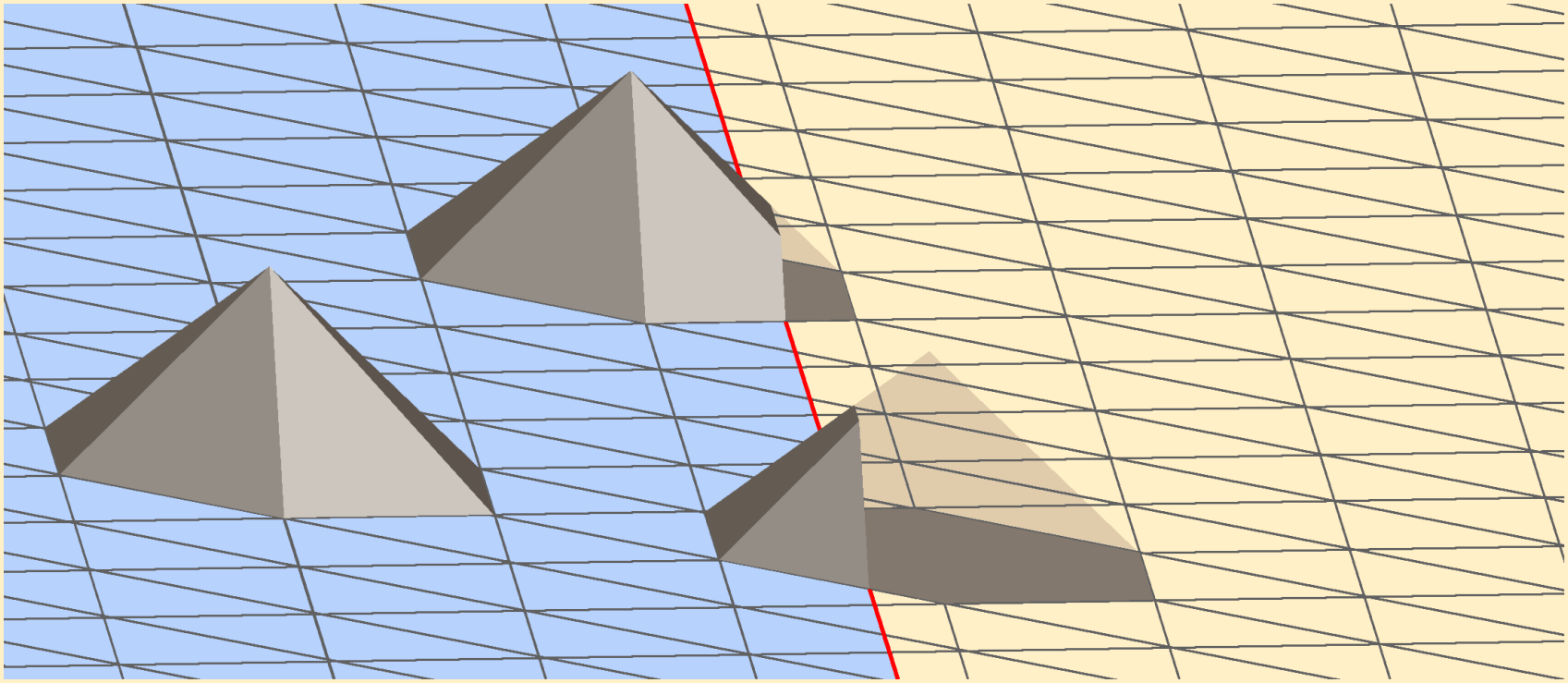

- far inside: standard tent
- at interface: truncated tent
- far outside: no tent

Spatial components of displacement are discretized separately

Standard vs. Composite Finite Elements

Finite Elements:

Standard vs. Composite Finite Elements

Finite Elements:

- structured cubic grids:
  - efficient
  - natural coarse scales
  - poor geometric flexibility

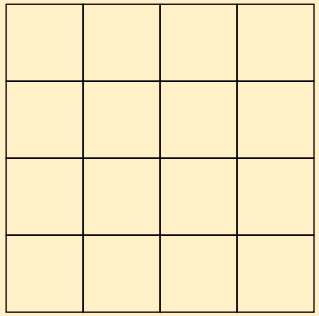

Standard vs. Composite Finite Elements

Finite Elements:

- structured cubic grids:
  - efficient
  - natural coarse scales
  - poor geometric flexibility
- unstructured triangular/tetrahedral grids
  - high geometric flexibility
  - meshing necessary
  - no natural coarse scales
  - key property: complicated grid with simple basis functions

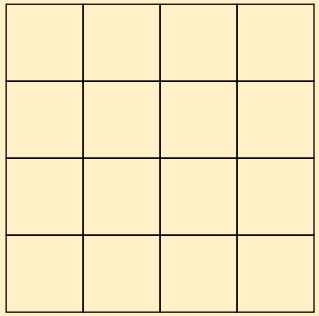

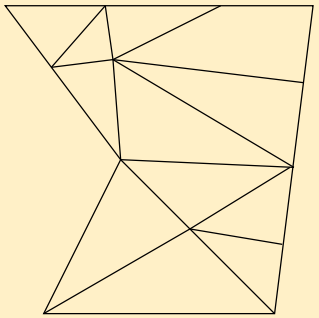

Standard vs. Composite Finite Elements

Finite Elements:

- structured cubic grids:
  - efficient
  - natural coarse scales
  - poor geometric flexibility
- unstructured triangular/tetrahedral grids
  - high geometric flexibility
  - meshing necessary
  - no natural coarse scales
  - key property: complicated grid with simple basis functions

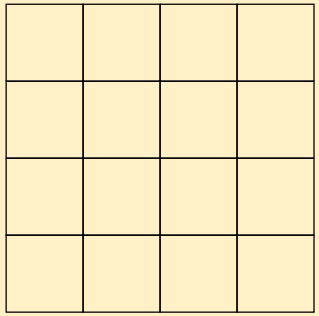

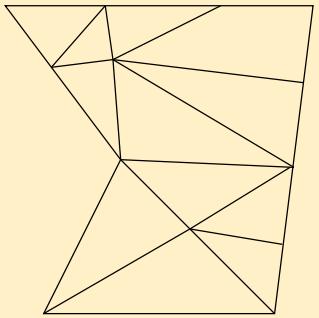

Composite Finite Elements:

- combine advantages of both

Standard vs. Composite Finite Elements

Finite Elements:

- structured cubic grids:
  - efficient
  - natural coarse scales
  - poor geometric flexibility
- unstructured triangular/tetrahedral grids
  - high geometric flexibility
  - meshing necessary
  - no natural coarse scales
  - key property: complicated grid with simple basis functions

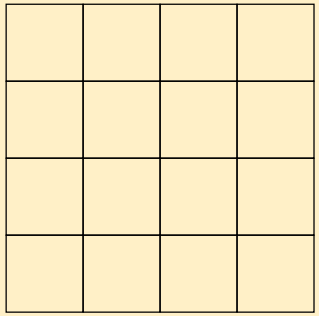

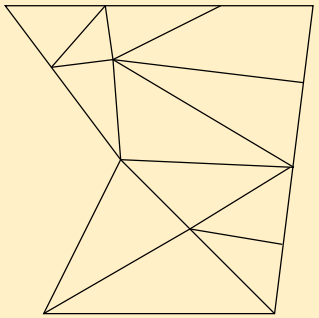

Composite Finite Elements:

- combine advantages of both

Standard vs. Composite Finite Elements

Finite Elements:

- structured cubic grids:
  - efficient
  - natural coarse scales
  - poor geometric flexibility
- unstructured triangular/tetrahedral grids
  - high geometric flexibility
  - meshing necessary
  - no natural coarse scales
  - key property: complicated grid with simple basis functions

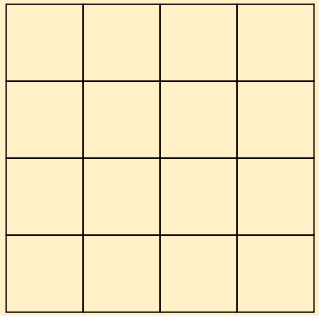

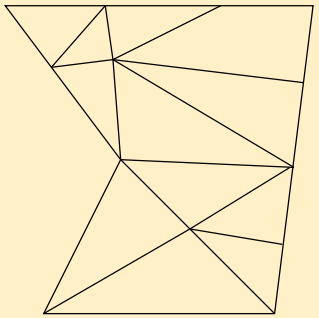

Composite Finite Elements:

- combine advantages of both
- use simple grid with complicated basis functions

Composite Finite Elements

- 3D: cubes, tetrahedra and more technical subdivision
- multigrid solvers possible
- discontinuous material coefficients across interface

Discretization of Periodic Boundary Conditions

- identification of DOF for nodes on opposite faces
- appropriate identification of basis functions
- CFE peculiarities

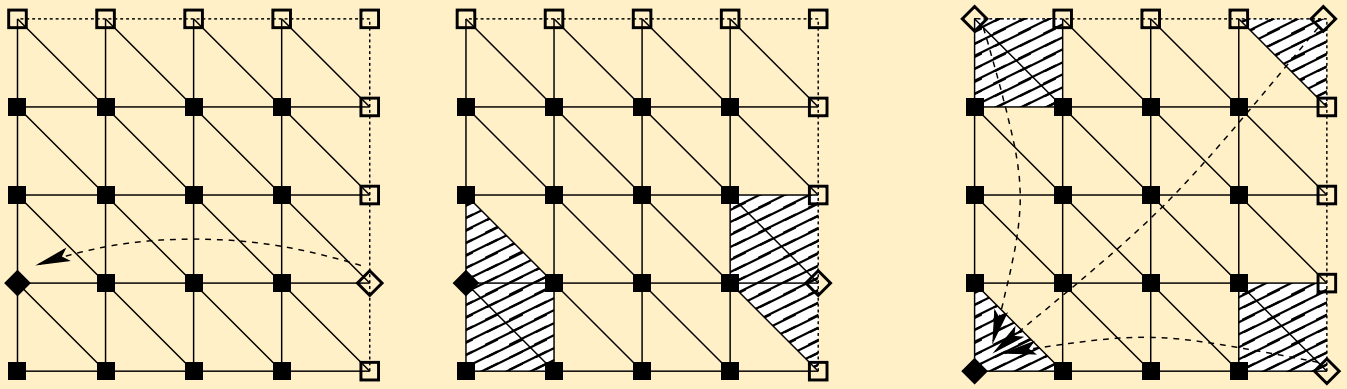

Contents

Periodic Specimen

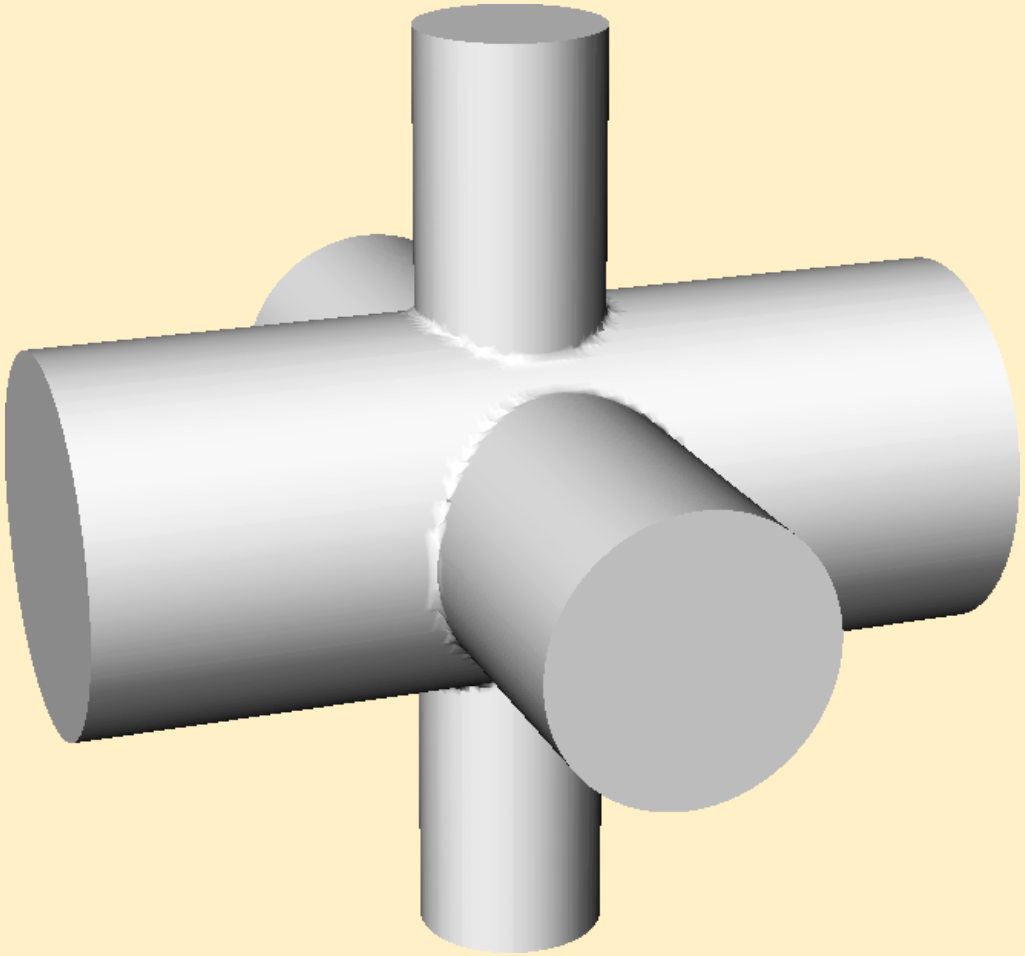

Diameter-to-length ratios $(0.4, 0.3, 0.2)$, $E = 100$ Pa, $\nu = 0.33$.

Results (Convergence)

Resolution 17^3:

$$\begin{bmatrix} 1.366 \cdot 10^{+01} & 1.337 \cdot 10^{+00} & 6.168 \cdot 10^{-01} & -2.335 \cdot 10^{-02} & -6.418 \cdot 10^{-03} & -1.175 \cdot 10^{-02} \\ 1.334 \cdot 10^{+00} & 8.261 \cdot 10^{+00} & 3.190 \cdot 10^{-01} & -4.811 \cdot 10^{-02} & 9.231 \cdot 10^{-03} & -1.754 \cdot 10^{-02} \\ 5.987 \cdot 10^{-01} & 3.082 \cdot 10^{-01} & 3.800 \cdot 10^{+00} & 6.818 \cdot 10^{-03} & -2.413 \cdot 10^{-04} & -1.821 \cdot 10^{-02} \\ -2.435 \cdot 10^{-02} & -5.255 \cdot 10^{-02} & 3.287 \cdot 10^{-03} & 9.040 \cdot 10^{-01} & 8.628 \cdot 10^{-03} & -4.890 \cdot 10^{-03} \\ -6.973 \cdot 10^{-03} & 8.953 \cdot 10^{-03} & 1.074 \cdot 10^{-03} & 8.253 \cdot 10^{-03} & 3.610 \cdot 10^{-01} & -2.262 \cdot 10^{-02} \\ -1.281 \cdot 10^{-02} & -1.716 \cdot 10^{-02} & -1.699 \cdot 10^{-02} & -6.356 \cdot 10^{-03} & -2.403 \cdot 10^{-02} & 2.331 \cdot 10^{-01} \end{bmatrix}$$

Results (Convergence)

Resolution 17^3:

$$\begin{bmatrix} 1.366 \cdot 10^{+01} & 1.337 \cdot 10^{+00} & 6.168 \cdot 10^{-01} & -2.335 \cdot 10^{-02} & -6.418 \cdot 10^{-03} & -1.175 \cdot 10^{-02} \\ 1.334 \cdot 10^{+00} & 8.261 \cdot 10^{+00} & 3.190 \cdot 10^{-01} & -4.811 \cdot 10^{-02} & 9.231 \cdot 10^{-03} & -1.754 \cdot 10^{-02} \\ 5.987 \cdot 10^{-01} & 3.082 \cdot 10^{-01} & 3.800 \cdot 10^{+00} & 6.818 \cdot 10^{-03} & -2.413 \cdot 10^{-04} & -1.821 \cdot 10^{-02} \\ -2.435 \cdot 10^{-02} & -5.255 \cdot 10^{-02} & 3.287 \cdot 10^{-03} & 9.040 \cdot 10^{-01} & 8.628 \cdot 10^{-03} & -4.890 \cdot 10^{-03} \\ -6.973 \cdot 10^{-03} & 8.953 \cdot 10^{-03} & 1.074 \cdot 10^{-03} & 8.253 \cdot 10^{-03} & 3.610 \cdot 10^{-01} & -2.262 \cdot 10^{-02} \\ -1.281 \cdot 10^{-02} & -1.716 \cdot 10^{-02} & -1.699 \cdot 10^{-02} & -6.356 \cdot 10^{-03} & -2.403 \cdot 10^{-02} & 2.331 \cdot 10^{-01} \end{bmatrix}$$

Resolution 33^3:

$$\begin{bmatrix} 1.280 \cdot 10^{+01} & 1.191 \cdot 10^{+00} & 5.881 \cdot 10^{-01} & 1.429 \cdot 10^{-03} & -4.527 \cdot 10^{-03} & -2.823 \cdot 10^{-03} \\ 1.203 \cdot 10^{+00} & 7.617 \cdot 10^{+00} & 3.064 \cdot 10^{-01} & -5.823 \cdot 10^{-03} & 3.690 \cdot 10^{-03} & -3.170 \cdot 10^{-03} \\ 5.877 \cdot 10^{-01} & 3.137 \cdot 10^{-01} & 3.964 \cdot 10^{+00} & 1.563 \cdot 10^{-03} & -1.666 \cdot 10^{-03} & -5.369 \cdot 10^{-03} \\ 1.200 \cdot 10^{-03} & -2.507 \cdot 10^{-03} & 5.538 \cdot 10^{-03} & 7.038 \cdot 10^{-01} & 3.277 \cdot 10^{-03} & -2.520 \cdot 10^{-03} \\ -4.967 \cdot 10^{-03} & 3.036 \cdot 10^{-03} & -1.412 \cdot 10^{-03} & 2.718 \cdot 10^{-03} & 2.691 \cdot 10^{-01} & -7.311 \cdot 10^{-03} \\ -2.770 \cdot 10^{-03} & -6.013 \cdot 10^{-03} & -6.026 \cdot 10^{-03} & -2.042 \cdot 10^{-03} & -7.838 \cdot 10^{-03} & 1.768 \cdot 10^{-01} \end{bmatrix}$$

Results (Convergence)

Resolution 17^3:

$$\begin{bmatrix} 1.366 \cdot 10^{+01} & 1.337 \cdot 10^{+00} & 6.168 \cdot 10^{-01} & -2.335 \cdot 10^{-02} & -6.418 \cdot 10^{-03} & -1.175 \cdot 10^{-02} \\ 1.334 \cdot 10^{+00} & 8.261 \cdot 10^{+00} & 3.190 \cdot 10^{-01} & -4.811 \cdot 10^{-02} & 9.231 \cdot 10^{-03} & -1.754 \cdot 10^{-02} \\ 5.987 \cdot 10^{-01} & 3.082 \cdot 10^{-01} & 3.800 \cdot 10^{+00} & 6.818 \cdot 10^{-03} & -2.413 \cdot 10^{-04} & -1.821 \cdot 10^{-02} \\ -2.435 \cdot 10^{-02} & -5.255 \cdot 10^{-02} & 3.287 \cdot 10^{-03} & 9.040 \cdot 10^{-01} & 8.628 \cdot 10^{-03} & -4.890 \cdot 10^{-03} \\ -6.973 \cdot 10^{-03} & 8.953 \cdot 10^{-03} & 1.074 \cdot 10^{-03} & 8.253 \cdot 10^{-03} & 3.610 \cdot 10^{-01} & -2.262 \cdot 10^{-02} \\ -1.281 \cdot 10^{-02} & -1.716 \cdot 10^{-02} & -1.699 \cdot 10^{-02} & -6.356 \cdot 10^{-03} & -2.403 \cdot 10^{-02} & 2.331 \cdot 10^{-01} \end{bmatrix}$$

Resolution 257^3:

$$\begin{bmatrix} 1.323 \cdot 10^{+01} & 1.213 \cdot 10^{+00} & 5.700 \cdot 10^{-01} & -3.114 \cdot 10^{-04} & -2.278 \cdot 10^{-04} & -1.702 \cdot 10^{-04} \\ 1.214 \cdot 10^{+00} & 8.149 \cdot 10^{+00} & 3.596 \cdot 10^{-01} & -7.628 \cdot 10^{-04} & 1.198 \cdot 10^{-04} & -2.541 \cdot 10^{-04} \\ 5.700 \cdot 10^{-01} & 3.588 \cdot 10^{-01} & 3.939 \cdot 10^{+00} & 1.441 \cdot 10^{-04} & -1.085 \cdot 10^{-04} & -4.061 \cdot 10^{-04} \\ -3.184 \cdot 10^{-04} & -6.852 \cdot 10^{-04} & 2.634 \cdot 10^{-04} & 6.620 \cdot 10^{-01} & 1.217 \cdot 10^{-04} & -6.435 \cdot 10^{-05} \\ -2.296 \cdot 10^{-04} & 1.266 \cdot 10^{-04} & -9.129 \cdot 10^{-05} & 1.225 \cdot 10^{-04} & 2.182 \cdot 10^{-01} & -3.005 \cdot 10^{-04} \\ -1.428 \cdot 10^{-04} & -2.450 \cdot 10^{-04} & -4.025 \cdot 10^{-04} & -5.785 \cdot 10^{-05} & -2.824 \cdot 10^{-04} & 1.718 \cdot 10^{-01} \end{bmatrix}$$

Rotated Artificial Periodic Object (Complicated Domain)

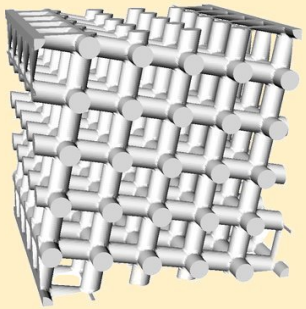

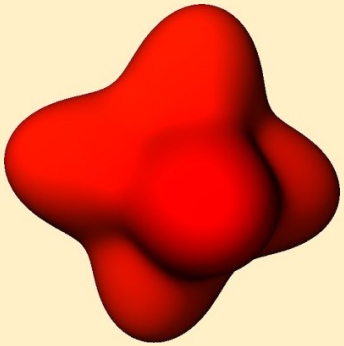

roll angle $= 11.31^\circ$

$$\bar{C} = \begin{bmatrix} 0.152681 & 0.019914 & 0.020399 & & & \\ 0.019914 & 0.140770 & 0.027324 & -0.017414 & & \\ 0.020399 & 0.027324 & 0.141225 & 0.017371 & & \\ & -0.017414 & 0.017371 & 0.022457 & -1.69 \cdot 10^{-4} & \\ & & & -1.69 \cdot 10^{-4} & 0.015305 & 2.18 \cdot 10^{-4} \\ & & & & 2.18 \cdot 10^{-4} & 0.014825 \end{bmatrix}$$

$$\bar{C}^Q = \begin{bmatrix} 0.152681 & 0.019962 & 0.020352 & -1.58 \cdot 10^{-4} & & \\ 0.019962 & 0.148068 & 0.020060 & & & \\ 0.020352 & 0.020060 & 0.148455 & & & \\ -1.58 \cdot 10^{-4} & & & 0.015193 & & \\ & & & & 0.015371 & \\ & & & & & 0.014759 \end{bmatrix}$$

(small entries have been omitted)

$(-11.33, 2.25 \cdot 10^{-3}, -1.72 \cdot 10^{-2})^\circ$

Non-Orthotropic Honeycomb Objects

Complicated domain:

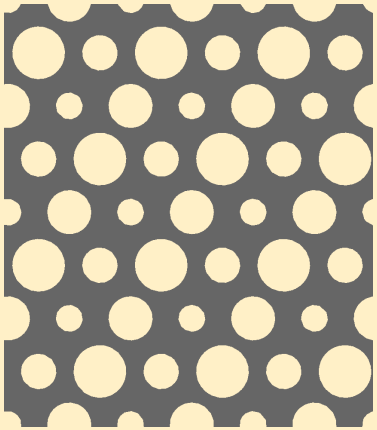

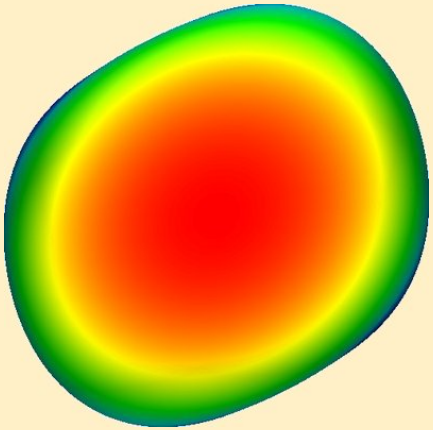

$$\bar{C}^{Q} = \begin{bmatrix} 4.172 & 1.899 & 2.307 & 1.22\cdot 10^{-10} & -7.58\cdot 10^{-10} & 0.125 \\ 1.899 & 3.451 & 2.033 & 4.53\cdot 10^{-10} & -3.57\cdot 10^{-10} & -0.051 \\ 2.307 & 2.033 & 6.499 & 4.20\cdot 10^{-10} & -1.32\cdot 10^{-09} & 0.028 \\ 1.22\cdot 10^{-10} & 4.53\cdot 10^{-10} & 4.20\cdot 10^{-10} & 1.179 & 0.036 & 1.22\cdot 10^{-13} \\ -7.58\cdot 10^{-10} & -3.57\cdot 10^{-10} & -1.32\cdot 10^{-09} & 0.036 & 1.337 & 8.44\cdot 10^{-11} \\ 0.125 & -0.051 & 0.028 & 1.22\cdot 10^{-13} & 8.44\cdot 10^{-11} & 1.085 \end{bmatrix}$$

Large optimal orthotropy violation (as expected).

Boundary Artifacts

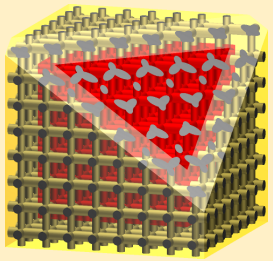

boundary layer β	$0/8$	$1/8$	$2/8$	$3/8$
relevant Frobenius difference	0.108	0.045	0.029	0.020
relative DOF usage	1.000	0.422	0.125	0.016

Trade-off between

- reduction of boundary artifacts
- computational efficiency

Specimen Acquisition

- Harvested vertebrae from spines of
  - young ♂ human
  - osteoporotic ♀ human
  - pig
  - cow

Specimen Acquisition

- Harvested vertebrae from spines of
  - young ♂ human
  - osteoporotic ♀ human
  - pig
  - cow
- physical preparation

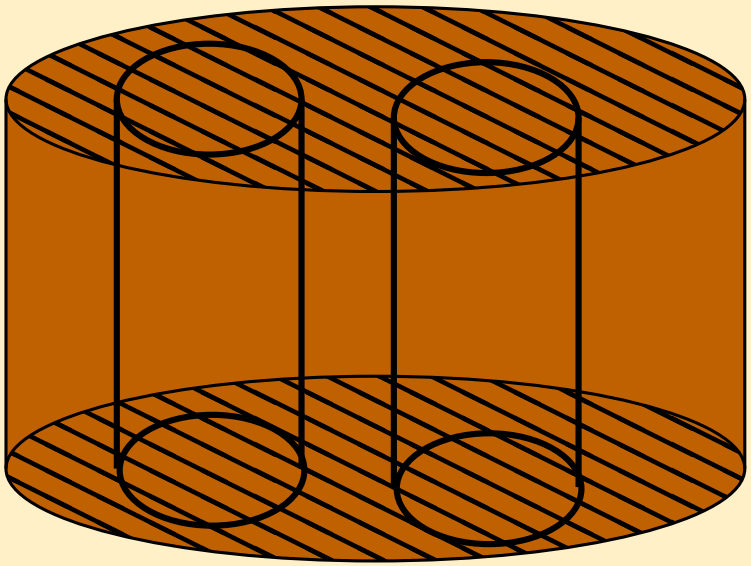

Specimen Acquisition

- Harvested vertebrae from spines of
  - young ♂ human
  - osteoporotic ♀ human
  - pig
  - cow
- physical preparation
- µCT scans at 40 µm
- cubic specimens of edge length 5.16 mm

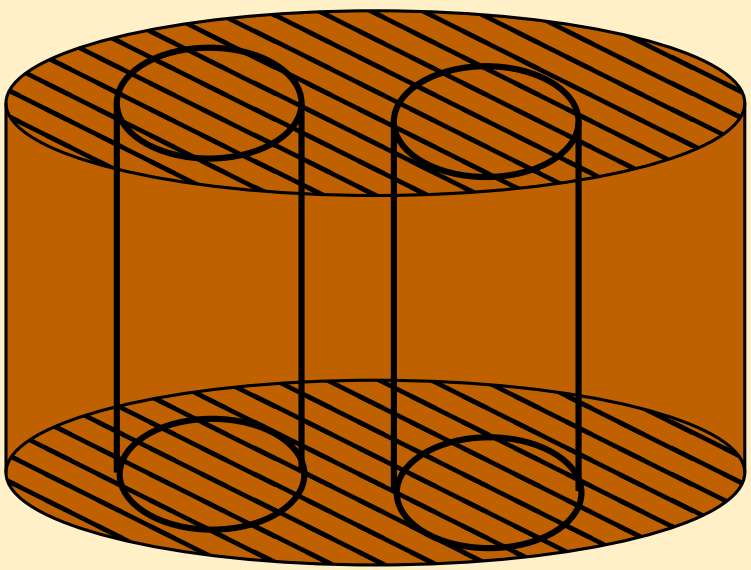

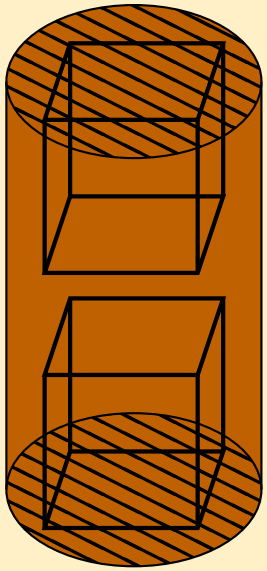

Results for Individual Specimens

human-y	human-o	porcine	bovine
♂ young	♀ osteoporotic		

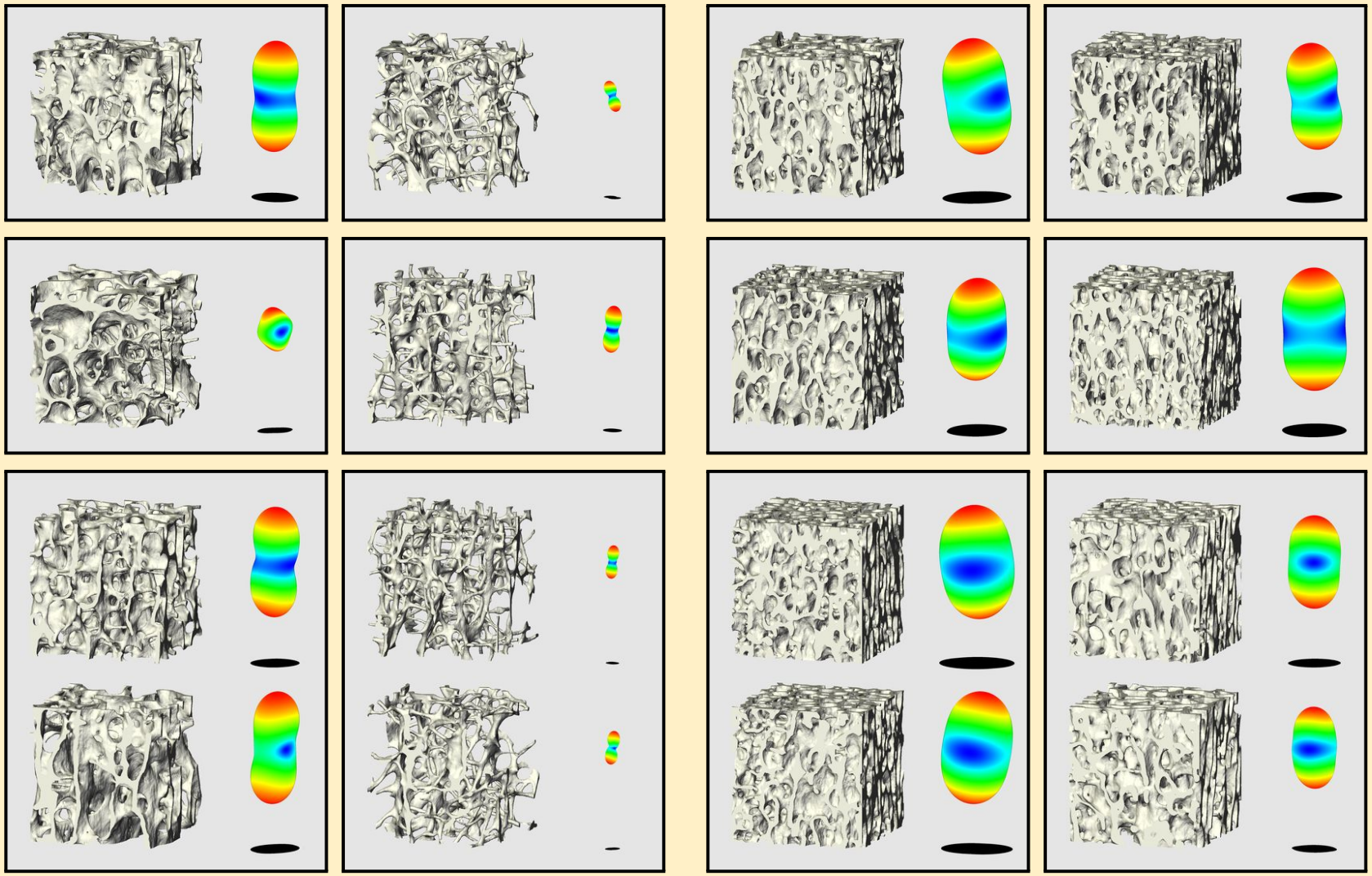

human tensors scaled by 4

Differences Between Species (Averages)

species	human-y	human-o	porcine	bovine
edge length of $\Omega^{\#}_{\beta=0.125}$ in Tb.Sp	4.22	3.65	9.08	7.90
volume fraction	0.141	0.081	0.370	0.330
E_{zz} in GPa	0.812	0.383	3.456	3.203
$\frac{E_{xx}+E_{yy}}{2}$ in GPa	0.334	0.130	1.831	1.263
anisotropy $\frac{2E_{zz}}{E_{xx}+E_{yy}}$	2.550	4.054	1.891	2.635

examples

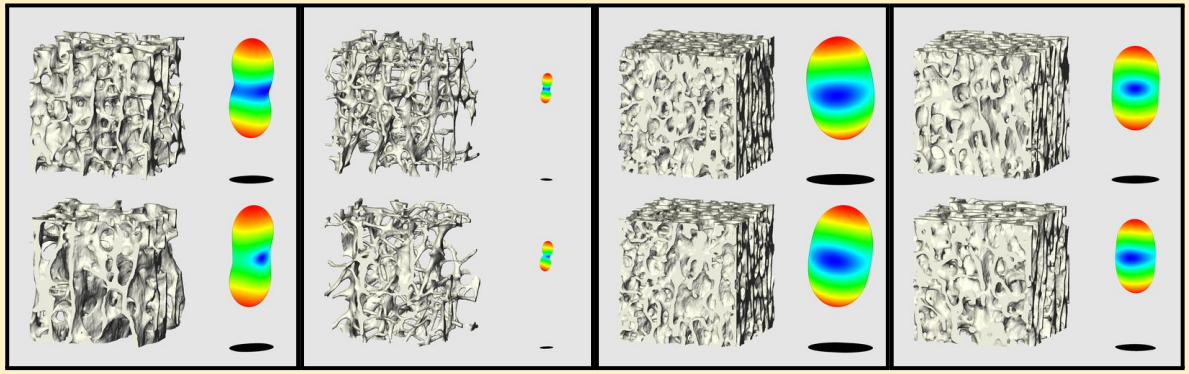

scaled by 4

z: aligned craniocaudal direction; x, y: aligned transverse directions

Differences Between Species (Averages)

species	human-y	human-o	porcine	bovine
edge length of $\Omega^{\#}_{\beta=0.125}$ in Tb.Sp	4.22	3.65	9.08	7.90
volume fraction	0.141	0.081	0.370	0.330
E_{zz} in GPa	0.812	0.383	3.456	3.203
$\frac{E_{xx}+E_{yy}}{2}$ in GPa	0.334	0.130	1.831	1.263
anisotropy $\frac{2E_{zz}}{E_{xx}+E_{yy}}$	2.550	4.054	1.891	2.635

examples

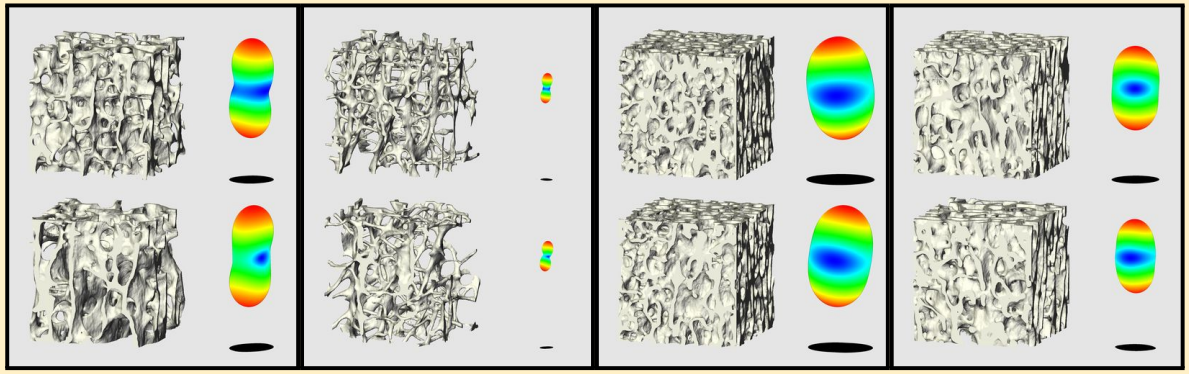

scaled by 4

z: aligned craniocaudal direction; x, y: aligned transverse directions

Differences Between Species (Averages)

species	human-y	human-o	porcine	bovine
edge length of $\Omega^{\#}_{\beta=0.125}$ in Tb.Sp	4.22	3.65	9.08	7.90
volume fraction	0.141	0.081	0.370	0.330
E_{zz} in GPa	0.812	0.383	3.456	3.203
$\frac{E_{xx}+E_{yy}}{2}$ in GPa	0.334	0.130	1.831	1.263
anisotropy $\frac{2E_{zz}}{E_{xx}+E_{yy}}$	2.550	4.054	1.891	2.635

examples

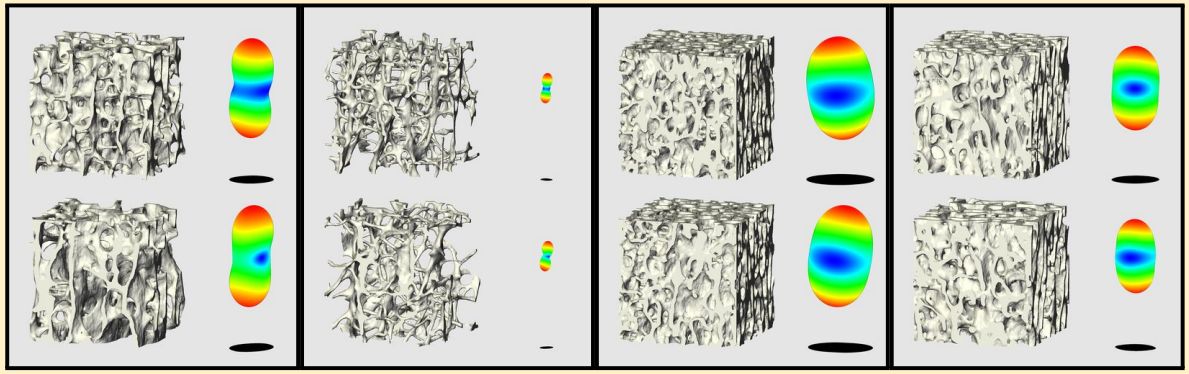

scaled by 4

z: aligned craniocaudal direction; x, y: aligned transverse directions

Differences Between Species (Averages)

species	human-y	human-o	porcine	bovine
edge length of $\Omega^{\#}_{\beta=0.125}$ in Tb.Sp	4.22	3.65	9.08	7.90
volume fraction	0.141	0.081	0.370	0.330
E_{zz} in GPa	0.812	0.383	3.456	3.203
$\frac{E_{xx}+E_{yy}}{2}$ in GPa	0.334	0.130	1.831	1.263
anisotropy $\frac{2E_{zz}}{E_{xx}+E_{yy}}$	2.550	4.054	1.891	2.635

examples

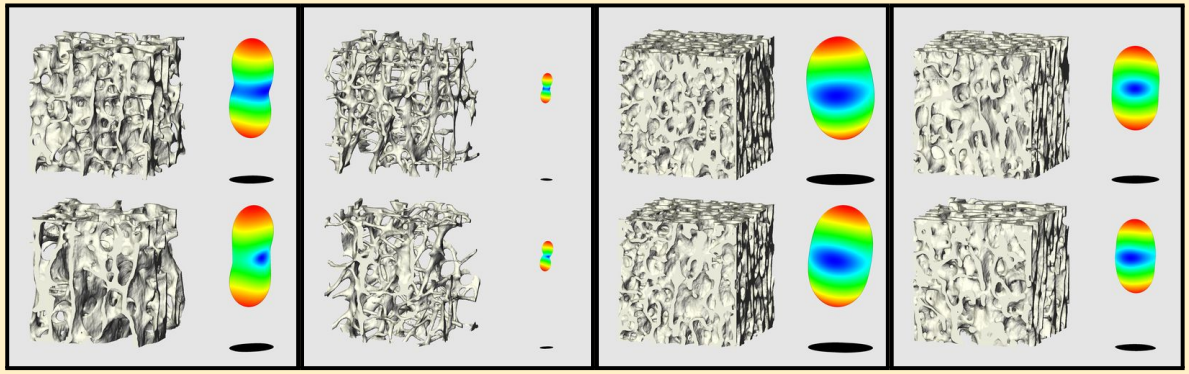

scaled by 4

z: aligned craniocaudal direction; x, y: aligned transverse directions

Differences Between Species (Averages)

species	human-y	human-o	porcine	bovine
edge length of $\Omega^{\#}_{\beta=0.125}$ in Tb.Sp	4.22	3.65	9.08	7.90
volume fraction	0.141	0.081	0.370	0.330
E_{zz} in GPa	0.812	0.383	3.456	3.203
$\frac{E_{xx}+E_{yy}}{2}$ in GPa	0.334	0.130	1.831	1.263
anisotropy $\frac{2E_{zz}}{E_{xx}+E_{yy}}$	2.550	4.054	1.891	2.635

examples

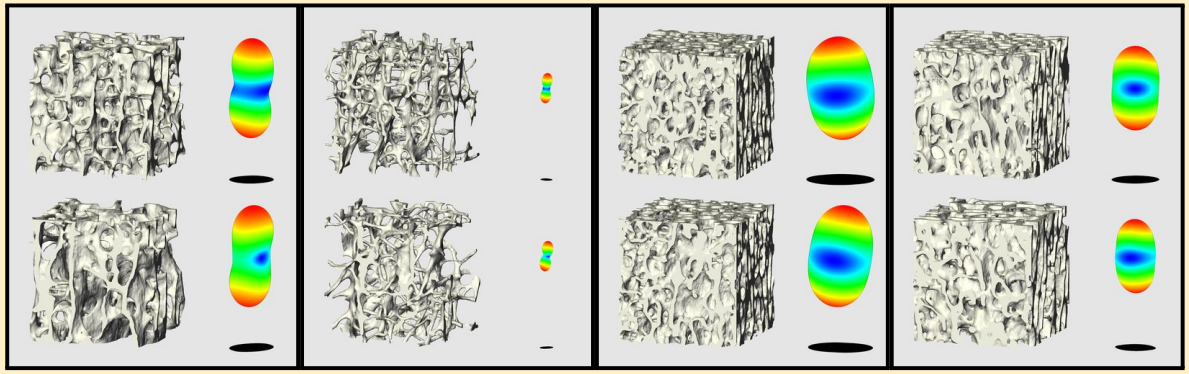

scaled by 4

z: aligned craniocaudal direction; x, y: aligned transverse directions

Differences Between Species (Averages)

species	human-y	human-o	porcine	bovine
edge length of $\Omega^{\#}_{\beta=0.125}$ in Tb.Sp	4.22	3.65	9.08	7.90
volume fraction	0.141	0.081	0.370	0.330
E_{zz} in GPa	0.812	0.383	3.456	3.203
$\frac{E_{xx}+E_{yy}}{2}$ in GPa	0.334	0.130	1.831	1.263
anisotropy $\frac{2E_{zz}}{E_{xx}+E_{yy}}$	2.550	4.054	1.891	2.635

examples

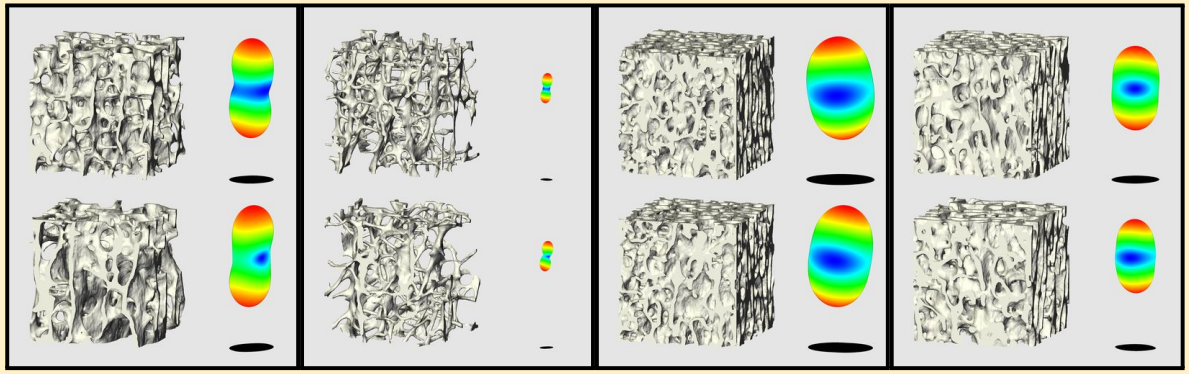

scaled by 4

z: aligned craniocaudal direction; x, y: aligned transverse directions

Differences Between Species (2)

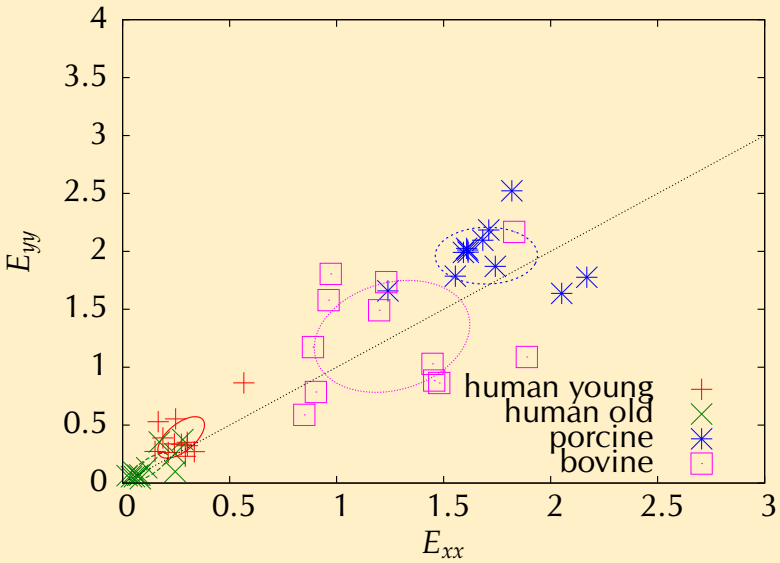

(ellipses: 1 standard deviation obtained by PCA)

Interpretation:

- transverse isotropy?

Differences Between Species (2)

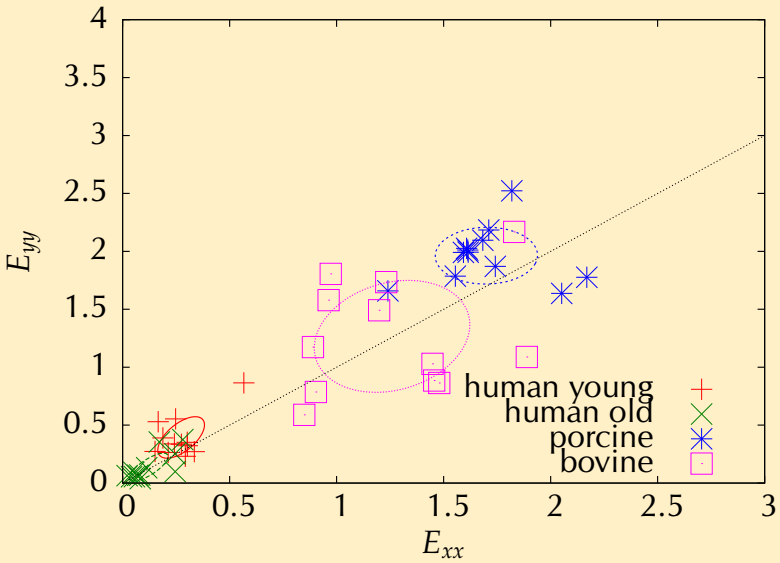

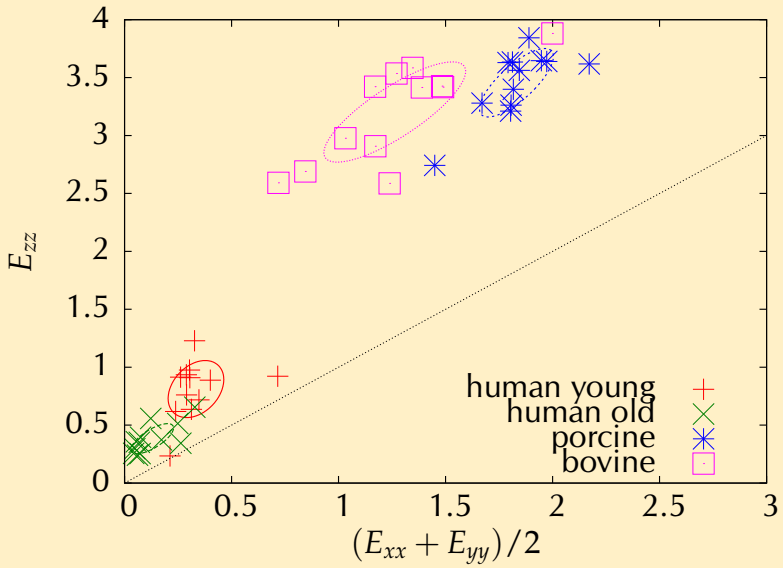

(ellipses: 1 standard deviation obtained by PCA)

Interpretation:

- transverse isotropy?
- anisotropy: craniocaudal/average transverse
- distinct clusters

Differences for a Single Vertebra

Need full two-scale model, cannot consider spongious interior as homogeneous material.

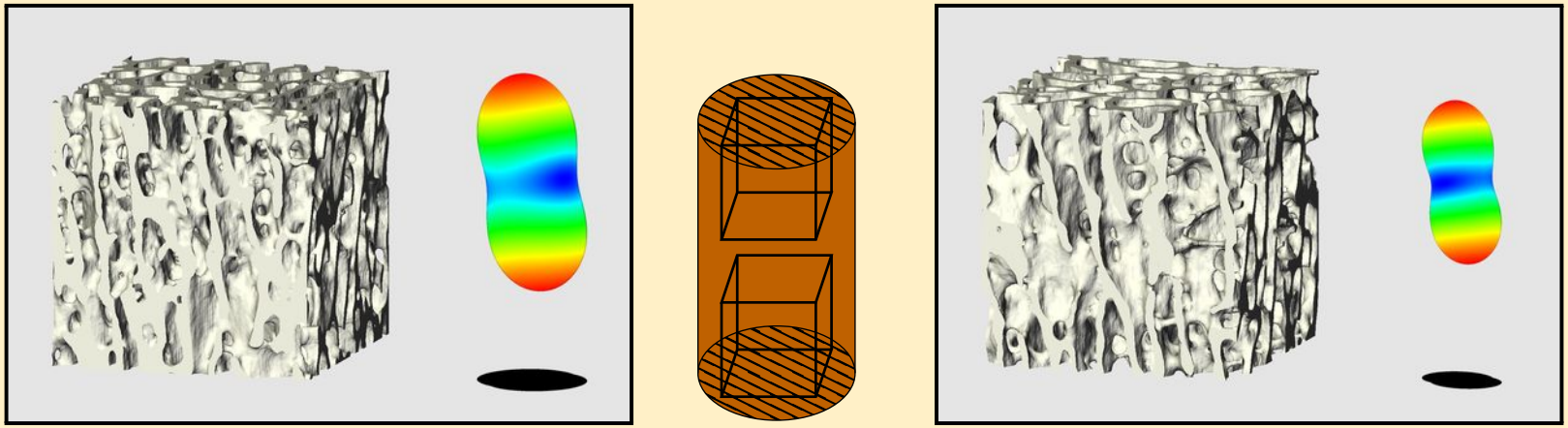

Differences for a Single Vertebra

Need full two-scale model, cannot consider spongious interior as homogeneous material.

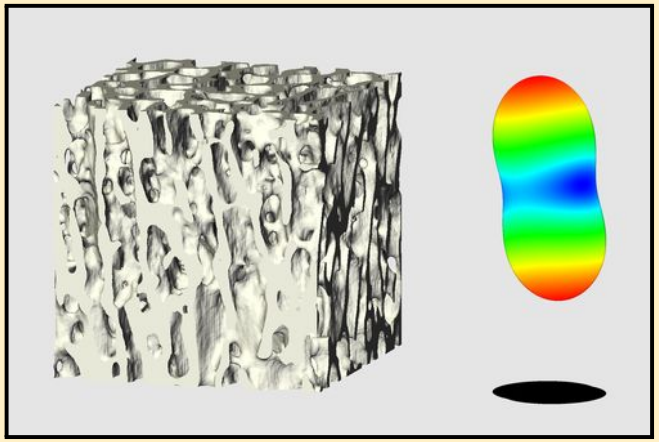

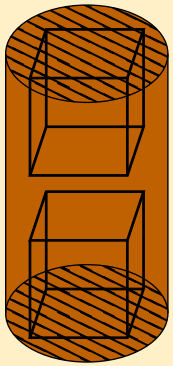

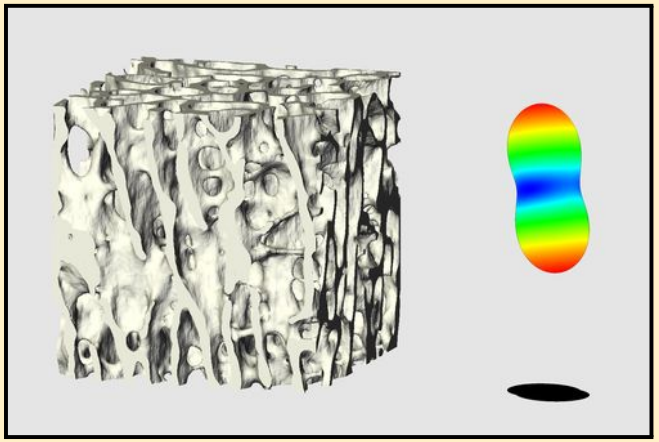

roll $= -7.52°$, pitch $= 9.44°$, yaw $= -18.22°$

$E_{xx} = 1.199$, $E_{yy} = 1.492$, $E_{zz} = 3.584$ GPa

roll $= -12.27°$, pitch $= 10.75°$, yaw $= -26.27°$

$E_{xx} = 0.903$, $E_{yy} = 0.786$, $E_{zz} = 2.690$ GPa

Summary

- homogenization method for periodic and statistically periodic trabecular microstructures
- some understanding of macroscopic properties of animal and human vertebral trabecular bone

Summary

- homogenization method for periodic and statistically periodic trabecular microstructures
- some understanding of macroscopic properties of animal and human vertebral trabecular bone
- limitations:
  - simple linear elasticity model (no plasticity or cracks)
  - uncertain material parameters (human vs. animal)
  - only 12 specimens per species
  - dorsoventral and dextrosinistral axes unknown
  - validation of Composite FE pending

References

- F. Liehr, T. Preusser, M. Rumpf, S. Sauter, and L. O. Schwen: *Composite finite elements for 3D image based computing*, Computing and Visualization in Science 12(4), pp. 171–188, 2009
- L. O. Schwen, U. Wolfram, H.-J. Wilke, and M. Rumpf: *Determining effective elasticity parameters of microstructured materials*, Proceedings of the 15th Workshop on the Finite Element Method in Biomedical Engineering, Biomechanics and Related Fields, University of Ulm, July 2008, pp. 41–62
- M. Rumpf, L. O. Schwen, H.-J. Wilke, and U. Wolfram: *Numerical homogenization of trabecular bone specimens using composite finite elements*, 1st Conference on Multiphysics Simulation – Advanced Methods for Industrial Engineering, Fraunhofer, 2010
- T. Preusser, M. Rumpf, S. Sauter, and L. O. Schwen, *3D composite finite elements for elliptic boundary value problems with discontinuous coefficients*, submitted to SIAM Journal on Scientific Computing

Contact: ole.schwen@mevis.fraunhofer.de